DOI:
10.1063/1.5085736

Document Version
Peer reviewed version

On the hydration of DOPE in solution

Natasha H. Rhys,[1,2,a)] Imogen B. Duffy,[1] Christopher L. Sowden,[1] Christian D. Lorenz,[2,b)] and Sylvia E. McLain[1,c)]

[1)] *Department of Biochemistry, University of Oxford, Oxford OX1 3QU UK*

[2)] *Department of Physics, King's College London, London, WC2R 2LS UK*

(Dated: 27 February 2019)

The atomic-scale hydration structure around the DOPE headgroup in a chloroform/water solution has been investigated using neutron diffraction enhanced by isotopic substitution and NMR, coupled with Empirical Potential Structure Refinement and Molecular Dynamics simulations. The results obtained show the preferential binding sites for water molecules on the DOPE headgroups, with the most predominant interactions being with the ammonium and phosphate groups. Interestingly, the level of hydration, as well as the association of DOPE molecules, varies according to the simulation method used. The results here suggest the presence of a tight water network around these lipid headgroups that could affect the permeability of the membrane for lipid-mediated diffusion.

PACS numbers: 61.20.-p

I. INTRODUCTION

The phosphatidylethanolamine (PE) headgroup is one of four primary headgroups for the phospholipids found in eukaryotic membranes. PE lipids comprise 75-80% of the total quantity of lipids in the inner membrane of *E. coli*,[1] 15-25% of the total quantity of lipids in eukaryotic membranes[2] and up to 45% of the total phospholipids in mammalian brains making them one of the major components of the brain endothelium cells and subsequently of the blood-brain barrier (BBB).[3] *In vivo*, PE lipids also serve as a precursor for the biosynthesis of PC lipids by a methyltransferase enzyme, where up to 30% of the PC lipids found in mammalian livers is thought to be produced via this process.[4]

Similar to the PC headgroup, PE lipids are zwitterionic. However, as opposed to the PC headgroup, PE is only zwitterionic when its terminal amine head group becomes protonated in solution. The presence of the -NH_3^+ ammonium group makes PE highly capable of hydrogen bond formation and adopting many different conformations relative to the membrane surface given its small size.[5] Within a membrane environment, PE lipids have been reported to form a conical shape - with the headgroup having a larger diameter towards the -PO_4^- phosphate portion of the phospholipid.[2] Since similar average conical structures are observed for many different types of lipids,[6] a more complete understanding of PE requires the detailed investigation of its underlying molecular interactions.

The interaction of water with the DOPE headgroup is of interest as the hydration of the lipid membranes has implications for disease control and cellular signaling. The interface between this hydrophilic environment with the hydrophobic membrane interior is where these interactions occur *in vivo*. Importantly, understanding the hydration of DOPE also has implications for drug delivery, particularly delivering drugs across the BBB where PE-phosopholipids are found in a relatively high proportion. Drugs have to be able to cross from an aqueous environment into and then through the hydrophobic interior of cellular membranes in order to function. A large proportion of BBB crossing drugs are thought to do so *via* lipid-mediated diffusion.[7,8] Understanding the hydration of the lipid head groups

[a)] natasha.rhys@kcl.ac.uk

[b)] chris.lorenz@kcl.ac.uk

[c)] sylvia.mclain@bioch.ox.ac.uk

This manuscript was accepted by J. Chem. Phys. Click here to see the version of record.

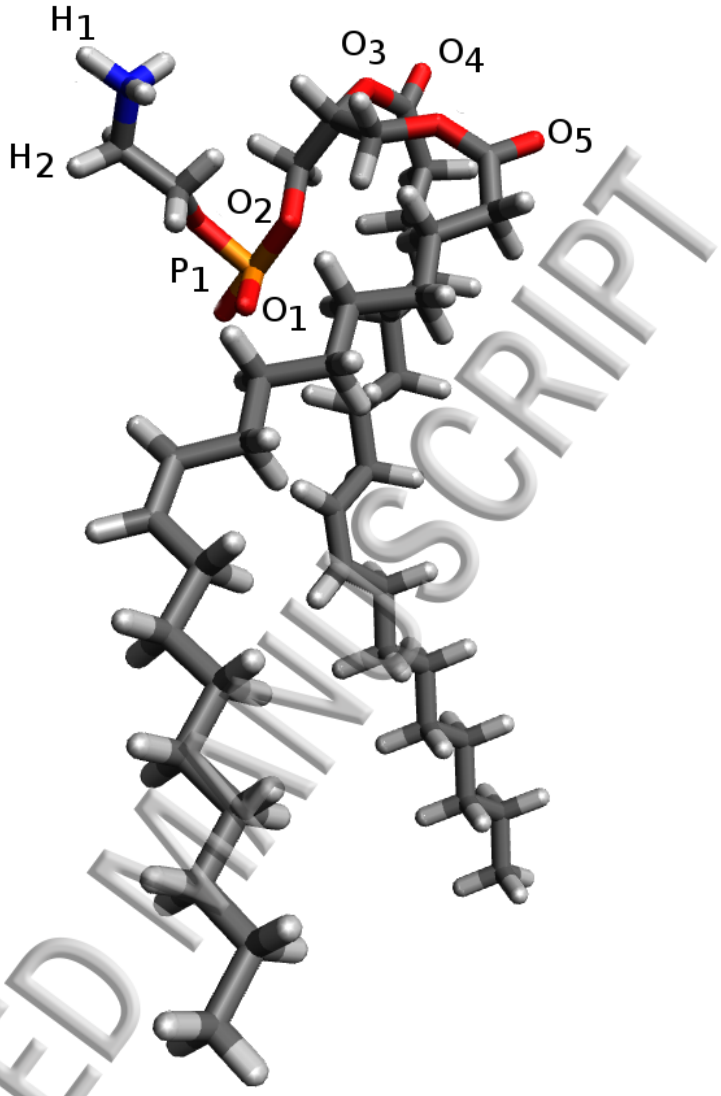

FIG. 1: Molecular structure of DOPE water with the atomic labels used in the EPSR simulation.

of the BBB can aid in the understanding of how molecules interact with these lipid moieties and importantly how water contributes to these interactions.

The present study aims to provide a site-specific atomic-scale description of the solvation of the DOPE lipid using a combination of neutron diffraction, NMR and computational techniques. In particular, the present investigation aims to determine how DOPE is preferentially hydrated in chloroform/water. While chloroform and water are generally not miscible, small quantities of water can be solubilized in chloroform[9], with the use of chloroform allowing for an understanding of the hydration of the head group without the complications of extensive lipid aggregation.[10] Importantly, it has been recently shown that hydration studies of headgroups in such solutions serve as a good predictor of the hydration behavior within a membrane.[11] This combination of experimental and computational techniques have also been used to characterize the hydration of other prominent lipid headgroups which are present within biological membranes - including the PC headgroup,[12–14] and the sphingolipid ceramide[10]. This multidisciplinary approach is ideal for determining the atomic scale interactions between lipids and the surrounding aqueous solvents.

TABLE I: Isotopomers of DOPE and water in chloroform solution measured by neutron diffraction

Sample	DOPE	Chloroform	Water
I	H	100% $CDCl_3$	H_2O
II	H	25% $CHCl_3$: 75% $CDCl_3$	H_2O
III	H	36% $CHCl_3$: 64% $CDCl_3$	H_2O
IV	H	50% $CHCl_3$: 50% $CDCl_3$	H_2O
V	H	75% $CHCl_3$: 25% $CDCl_3$	H_2O
VI	H	100% $CHCl_3$	H_2O

II. METHODS

A. Sample preparation

1,2-dioleoyl-sn-glycero-3-phosphoethanolamine (DOPE) was purchased from Avanti Polar lipids and was used without any further purification, and stored in a freezer (-20^{o}C) in a N_2 filled glove box. Chloroform ($CHCl_3$) and deuterated chloroform ($CDCl_3$) were both purchased from Sigma Aldrich and dried by refluxing over CaH_2 at ∼50^{o}C for 24-48 hours, then cryogenically distilled *in vacuo* and stored over molecular sieves. Both $CHCl_3$ and $CDCl_3$ were verified as anhydrous by ^{1}H NMR, with no water peaks present in the spectra for each dried solvent.[15]

B. NMR

NMR measurements were completed using a Bruker 500 MHz instrument, from the biomolecular NMR facility at the University of Oxford. ^{1}H, COSY and NOESY NMR spectra were collected for DOPE in anhydrous $CDCl_3$ as well as for DOPE/$CDCl_3$ solutions with water added in stoichiometrically under a N_2-flow, with final stoichiometric ratios of 1:2:300, and 1:5:300 DOPE:water:$CDCl_3$.

C. Neutron diffraction

Neutron diffraction with isotopic substitution experiments were performed on six isotopomeric samples of DOPE in water/chloroform solutions using the SANDALS diffractometer located at the ISIS neutron facility (STFC, UK). These samples, listed in Table I, have varying proportions of hydrogen and deuterium within the sample, with each having a final molecular ratio of 1 DOPE : 5 water : 300 chloroform. For the experiments, DOPE and chloroform were transferred by weight in gas-tight vials, within a N_2-filled glove box. Water was then added, by volume to obtain the solutions listed in Table I. The samples were subsequently transferred for the experiments to Ti/Zr alloy, flat-plate cans with a sample thickness of 1 mm, to minimize multiple scattering for the protiated samples. All experiments were performed at standard temperature and pressure.

Diffraction data were collected for each solution for an average of ∼8 hours (∼1000 μA). Using the Gudrun software[16], each dataset was corrected for background, multiple scattering and absorption effects, and normalized using a vanadium standard.

The diffraction experiment yields the total static structure factor for each sample, $F(Q)$, which measures every individual pair correlation in the solution in reciprocal space:

$$F(Q) = \sum_{\alpha,\beta \geq \alpha} (2 - \delta_{\alpha\beta}) c_\alpha \, c_\beta \, b_\alpha \, b_\beta \, (S_{\alpha\beta}(Q) - 1) \qquad (1)$$

Here, c is concentration of atoms α and β, b is the coherent neutron scattering length of,[17] while $S(Q)$ equates to the elastic scattering vector $Q = 4\pi \sin(\theta)/\lambda$. Each of the individual pair correlation functions, $S_{\alpha\beta}(Q)$ form a Fourier pair with their specific radial distribution functions (RDF; $g_{\alpha\beta}(r)$) which yields real-space atomic distances:

$$S_{\alpha\beta}(Q) = 1 + \frac{4\,\pi\,\rho}{Q} \int r\,[(g_{\alpha\beta}(r) - 1)]\,\sin(Qr)\,\mathrm{d}r \tag{2}$$

As the diffraction patterns are normalized and the density of the solution known, integration of the individual $g_{\alpha\beta}(r)$s within a given distance range r_1 and r_2 provides the average coordination for the interactions between the atom pairs in the solution:

$$n_{\alpha}^{\beta} = 4\pi\rho c_{\beta} \int_{r_1}^{r_2} r^2 g_{\alpha\beta}(r)\,\mathrm{d}r \tag{3}$$

D. Empirical Potential Structure Refinement

While it is possible in cases, where there are a small number of atoms, to extract the individual site-site $S_{\alpha\beta}(Q)$ by combining diffraction patterns from several isotopically-labeled solutions,[18] for solutions containing a large number of distinct atoms this is not possible or practical. As a result, Empirical Potential Structure Refinement (EPSR) simulations were employed, where this Monte Carlo-based simulation technique has been specifically designed to generate a computational model of a disordered system which fits a set of measured diffraction data in order to extract a full set of correlations for any given system.[19,20] This analysis method has been used to explore a range of chemical and biological solutions,[21–30] as well as specifically for the hydration of lipid molecules.[10,12–14,31]

Here EPSR simulations were performed on a box containing 10 DOPE, 50 H_2O and 3000 $CHCl_3$ molecules at the temperature and atomic number density of the measurement (298 K and 0.0374 atoms/Å^3). The reference potentials used for DOPE (listed in Table I of the SI) are from the CHARMM36 forcefield[32] with its intramolecular geometry taken from the CHARMM-GUI online resource.[33,34] The SPC/E potentials were used for the water molecules[35], whilst chloroform was modeled using the OPLS potentials[36]. It should be noted that EPSR does not provide a unique solution for the system in question but does provide a model that is consistent with a set of measured data and will be somewhat dependent on the seed potential values, especially when these correlations are not well represented in any measured data set. The fits to the measured $F(Q)$ data and the difference between data and fit are shown in Fig. 2, with the real-space version, $G(r)$, shown in Figure 1 (b) of the SI.

E. Molecular Dynamics

Molecular Dynamics (MD) simulations were also performed for DOPE in solution at the same composition and ratio of molecules (10 DOPE molecules, 50 water molecules and 3000 chloroform molecules) as for the EPSR simulations of the neutron diffraction data. The DOPE molecules were modeled using the CHARMM36 forcefield[32] and the water molecules were modeled with the TIP3P model[37] which has been modified for the CHARMM force field.[38] While this differs from the potentials used for EPSR, no major discrepancies between simulation results have been reported in previous studies on lipids from this, including when water is the bulk solvent.[12–14] The chloroform molecules were modeling using a model originally parameterised for the OPLS/AA forcefield[39], which have been used in previous simulations of ceramide lipids in water and chloroform.[10] All of the bonds and angles for the water molecules were constrained using the SHAKE algorithm[40].

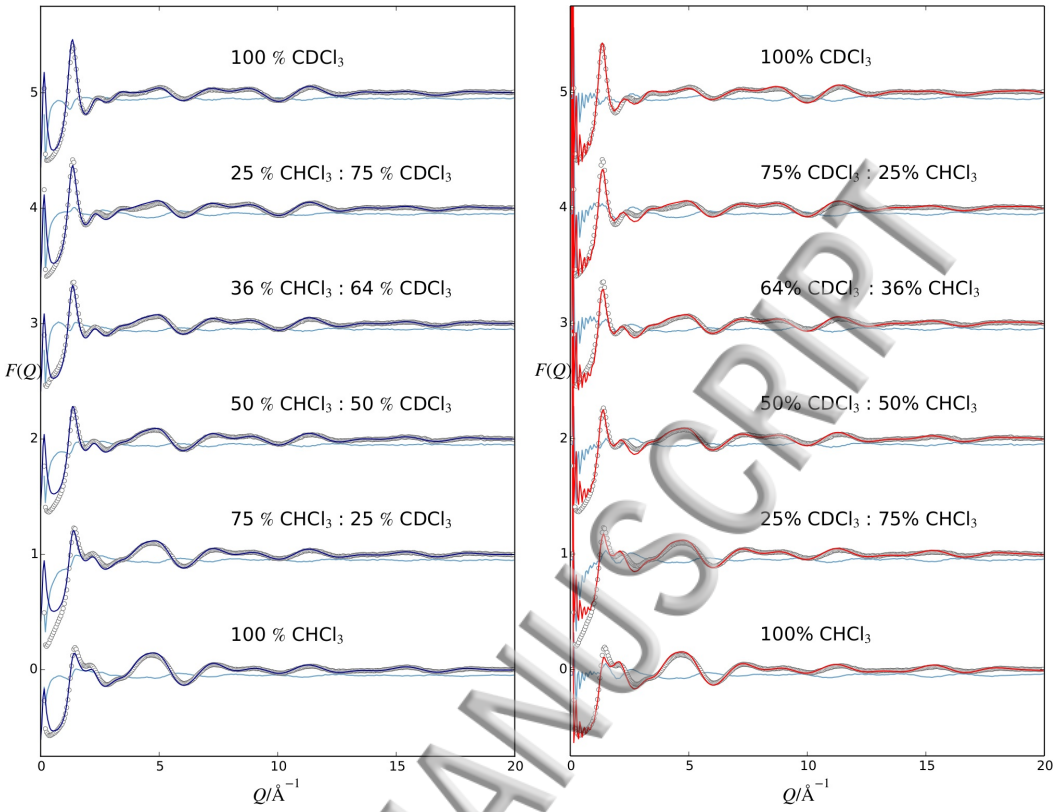

FIG. 2: The $F(Q)$ fits for EPSR (left, blue line) and MD (right, red line) to the measured diffraction data (gray circles), as well as the difference between the fit for each simulation and the data (pale blue line) for each of the measured DOPE/water/chloroform solutions. Each dataset has been offset by 1 for clarity.

The volume of the system was equilibrated at 300 K and 1 atm using the NPT ensemble for approximately 1 ns, the subsequent production simulations were performed using the NPT ensemble at 300 K and 1 atm and run for 100 ns. All simulations were conducted using the LAMMPS MD code[41] and a 2.0 fs timestep with the velocity Verlet integrator was used. The Nosé-Hoover thermostat and barostat, as they are implemented in LAMMPS, were used. The van der Waals interactions were cut-off at 12 Å, and the PPPM algorithm[42] was used to compute the long-range Coulombic interactions. The $F(Q)$s calculated from the MD simulation compared to the measured NDIS data are shown in Figure 2(b), whilst the Fourier transformation of the simulated $F(Q)$ are shown in Fig. SI.1(b) of the Supplementary Information.

In order to investigate the binding of water to different parts of the DOPE lipid head groups, the survival probability of water molecules were measured that are within the first neighbor distance as determined from the RDF of the oxygen atom in a water molecule around the different headgroups. Such analyses have been used previously to understand the hydration of cocaine in aqueous and chloroform solutions.[43] In doing so, the time that each water molecule within the hydration shell stays within the hydration shell before leaving is measured. From this, it possible to calculate the probability that a hydrating water molecule stays within the hydration shell for a given time τ.

Also, this study has investigated the role that water plays in bridging different parts of the lipid head groups within the same molecule and between two different lipid molecules. In doing so, a graph-theoretic (GT) approach is used to investigate the topological structure of interactions between the amine, phosphate and ester groups within the headgroup of

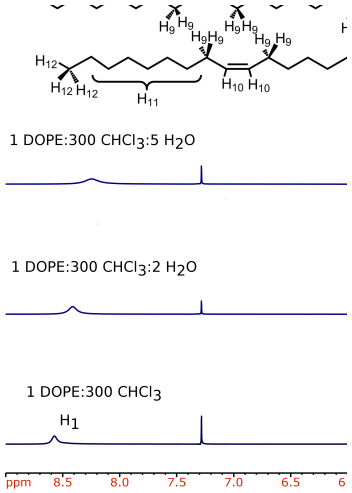

FIG. 3: ^{1}H NMR spectra for DOPE in $CDCl_3$ solutions, in the absence of water, and with 2 and 5 parts water per DOPE. Labeling for the DOPE protons is shown in the inset and the spectra have been offset for clarity.

the DOPE lipid molecules. This GT approach is based upon an in-house code that takes advantage of some of the functionality of the *NetworkX* Python library.[44] Using this code, the MD trajectory dynamics are mapped to an ensemble of unweighted, undirected graphs $G(V, E)$. At each timestep, a graph is formed consisting of a number of vertices (V), which each represent a single H2O molecule or one of the groups within a lipid headgroup. Hydrogen bonds, as defined empirically, form the edges (E) of the graph. The graph structure is contained in an adjacency matrix $\mathbf{A}$, where:

$$[\mathbf{A}]_{ij} = \begin{cases} 1, & \text{if } i \text{ and } j \text{ are connected} \\ 0, & \text{if } i \text{ and } j \text{ are not connected.} \end{cases}$$

In a similar way to previous work[14,45], the GT framework is used to calculate the probability distribution of shortest through-water paths from each group in a lipid headgroup to any other group in a lipid headgroup. Then the probability distributions of the measured minimum paths connecting two groups in the PE headgroup on the same or different lipid molecules are determined.

F. ANGULA

Both the EPSR modeling box and the MD trajectories were further analyzed using the software ANGULA.[46,47] Here, a set of orthonormal coordinates were assigned to both the water molecules, chloroform and different portions of the DOPE molecules (see SI Figure 2) to assess the 3-dimensional hydration structure around the DOPE headgroup by virtue of Spatial Density Maps (SDMs) *vide infra*. For EPSR, 5312 configuration files were collected for the subsequent analysis and 4005 snapshots of the MD trajectory were used as a comparison, comparable to number of frames used in ANGULA analyses on other lipids[11,14]. The maps show the location of molecules around a central group, with the scale bar representing the density of atoms per Å^3 for a specified distance range and percentage.

III. RESULTS AND DISCUSSION

A. NMR of DOPE

Figure 3 shows the ^{1}H NMR for DOPE in anhydrous $CDCl_3$ and for the same solution with 2 and 5 molar equivalents of water added with the molecular labeling added as a reference. The water resonance appears as a singlet peak at 2.95 ppm in the 1:2 DOPE:water sample, which shifts further downfield to 3.40 ppm in the 1:5 sample. As a comparison, the water resonance in $CDCl_3$ appears at 1.56 ppm in the absence of DOPE,[15] and in the present solution shows a much larger downfield shift than was observed for water in ceramide/chloroform solutions.[10] This significant downfield shift for water in this solution is likely due to the formal charge on the -NH_3^+ motif for DOPE and suggests that water is relatively tightly bound to the DOPE lipid rather than being isolated from the lipid in solution.

For DOPE, the addition of water to the solution results in a broadening and an upfield shift of the -NH_3^+ resonance (H_1; Fig. 1) from 8.56 to 8.41 ppm with 2 molar equivalents of water and to 8.23 ppm upon the addition of 5 molar equivalents of water. While the broadening of this peak is a result of exchange between water and the -NH_3^+ hydrogen atoms, the upfield shift suggests that these hydrogen atoms become more shielded due to the -NH_3^+-water coordination diminishing the effective charge on the nitrogen atom. While hydrogen bonding typically results in a downfield shift due to the proton becoming deshielded, the reduction in electronegativity of the nitrogen atom could likely counter the effects of this resulting in only a small reduction in the chemical shift.

For the other DOPE resonances, there are only very slight shifts upon the addition of water. The H2 resonance shows a small downfield shift, and the H4' and H3 peaks at around 4.1 ppm become more well separated as the concentration of water increases. These peak shifts are likely a result of a slight change in the polarity of the DOPE molecule. This change in polarity is probably due to water binding to the phosphate group as it is relatively close in proximity to these hydrogen atoms.

In addition to the 1D experiments shown in Fig. 3, 2D ^{1}H-^{1}H NOESY correlation spectra were recorded for the same solutions, to ascertain the connectivity between water and the DOPE molecule. Figure 4 shows the ^{1}H-^{1}H NOESY spectrum for DOPE in $CDCl_3$ with the addition of 5 molar equivalents of water. For reference, the comparable spectrum for DOPE in $CDCl_3$ with all cross-peak labels, is presented in Figure 3 of the SI. From this spectrum, it is clear that water readily interacts with the H1 protons, shown by a cross-peak present at 3.13 ppm and 8.23 ppm, corresponding to the chemical shifts for water and the H1 protons respectively. This correlation on Figure 4 is marked by red lines. Furthermore, a NOESY correlation indicating hydration interactions is found between the H_2 hydrogen atoms in DOPE and water, corresponding to the -CH_2CH_2- hydrogens directly below the -NH_3^+ group(Fig. 1). Similar NOESY experiments show the presence of comparable alkene hydrogen water bonding in ceramide[10], which through diffraction and computational studies has also been shown to occur for the PC headgroup in solution[12–14] and in a bilayer environment.[11] This 2D spectrum taken together with the ^{1}H spectra shown in Fig. 3 suggest that the water molecules are bound rather tightly to the -NH_3^+ headgroup and are not isolated from the DOPE molecule in the solutions. Additionally, it shows that the water molecules are tightly bound to DOPE, exchanging relatively little with one another as the water-DOPE correlation in NOESY spectra is visible, where in the case of fast exchange between two molecules there would be an absence of cross peaks between the Hw and H_1 protons in the solution.

B. Association of DOPE

Figure 5 shows the inter-molecular interactions of the ammonium hydrogen with phosphate and ester oxygens on neighboring DOPE molecules. In all cases, DOPE-DOPE asso-

This manuscript was accepted by J. Chem. Phys. Click here to see the version of record.

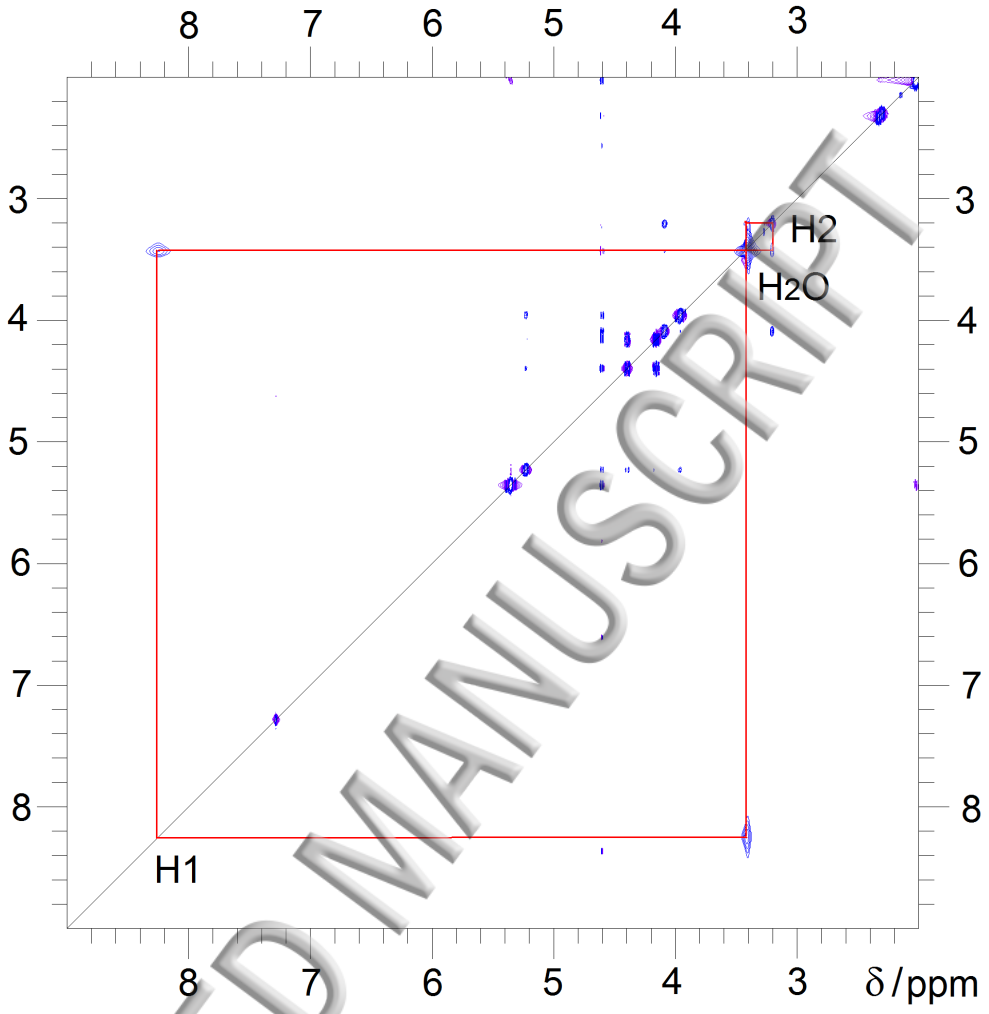

FIG. 4: ^{1}H-^{1}H NOESY correlation spectra for DOPE in $CHCl_3$ (red) and with the addition of 5 parts water (blue).

ciation predominates in MD compared to EPSR. With the exception of H1-O5 interactions, where the coordination numbers (Table II) for each simulation are both 0.04, the coordination for DOPE-DOPE contacts found in the MD simulations are typically 4-5 times the value of those from EPSR. The total number of hydrogen bonds between DOPE lipids has been previously reported by Sodt and Pastor,[48,49] which was reported as 0.75 for planar and increases upon inducing curvature.

To understand the DOPE-DOPE interactions present in the MD simulation, Figure 6 first shows the probability distributions of two different parts of the DOPE headgroup being linked either directly or by a hydrogen-bonded chain of water molecules of a certain length. In Fig. 6(a), the probability distributions are shown for NH_3^+-NH_3^+, phosphate-phosphate, and ester-ester groups on two different DOPE molecules. The ammonium and phosphate groups are most commonly bonded by a single water molecule, whereas the ester groups are most commonly connected through 3 water molecules where this distribution is much broader.

Figs. 6 (b)-(d) show the MD probability distributions of direct interactions and hydrogen-bonded water molecule chains connecting intramolecular and intermolecular NH_3^+-phosphate,

This manuscript was accepted by J. Chem. Phys. Click here to see the version of record.

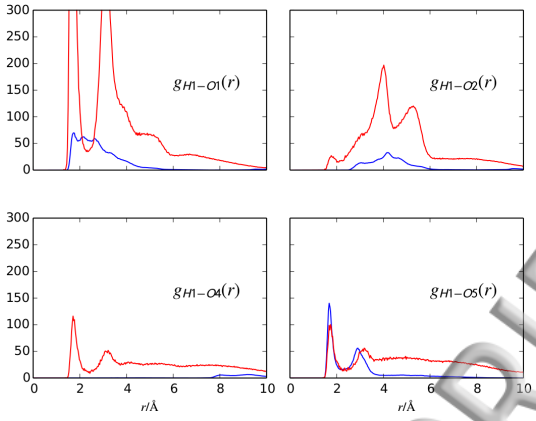

FIG. 5: The $g(r)$s for the DOPE-DOPE headgroup intermolecular interactions in solution for the EPSR (blue) and MD (red) simulations.

	r_{min}/Å	EPSR	MD
H1-O1	2.40	0.1	0.5
H1-O2	2.40	0	0.04
H1-O4	2.40	0	0.04
H1-O5	2.40	0.04	0.04

TABLE II: Coordination numbers for the DOPE-DOPE intermolecular $g(r)$s in Figure 5.

NH_3^+-ester, and phosphate-ester pairs, respectively. For the NH_3^+-phosphate pairs, when these groups are on different DOPE molecules, they interact most commonly via direct interactions, whereas these two groups on the same molecule are more commonly linked by one water molecule. Conversely, while there are a significant number of direct intermolecular interactions between the ammonium and ester groups, the intermolecular ammonium-ester groups are most commonly found to be linked via one water molecule. There is very rarely a hydrogen-bonded network connecting the ammonium and ester groups on the same molecule, and when there is, it is equally likely to contain between 1 and 3 water molecules. The phosphate-ester pairs are the only ones where the most probable hydrogen-bonded path connects intramolecular interactions, which most commonly contain 1 water molecule.

To investigate the potential causes of the aggregation observed in MD, simulations have also been completed to understand the inter- and intramolecular interactions between the various parts of the DOPE headgroup in a system with a ratio of 1:2 DOPE molecules to water molecules, as opposed to 1:5. The probability distributions for the interactions between each pair of groups for the 1:2 simulation is shown in SI Figure 10. While the size of clusters increase to a comparable size for each simulation (see SI Figures 8 & 9), there is an increased preference for the lipid headgroups to interact, whether it be via direct or water-mediated interactions, in the 1:2 system as compared to the results shown in Fig. 6. Therefore this association of the lipid molecules observed in simulations seems to be quite sensitive to the number of water molecules present in the system.

C. Hydration of DOPE

The distribution of water survival probabilities around the NH_3^+, phosphate and ester groups of the DOPE lipid headgroup are shown in Figure 7. The results show that the water molecules are more likely to remain bound to the ammonium and phosphate groups for longer times than the water molecules bound to the ester groups. While there is a slight difference in the half-life of a water molecule around the phosphate and ammonium

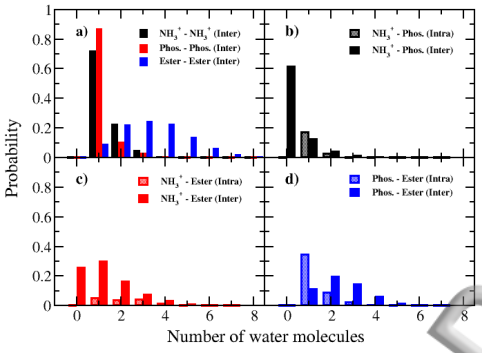

FIG. 6: Probability distributions of various parts of the DOPE headgroup being linked through hydrogen-bonded chains containing a given number of water molecules. The four graphs show the probability distributions of the number of water molecules that link (a) the same part of the headgroup on two different molecules, (b) the intra- and intermolecular interactions of the -NH_3^+ & phosphate groups, (c) the intra- and intermolecular interactions of the -NH_3^+ & ester groups, and (d) the intra- and intermolecular interactions of the phosphate & ester groups.

groups (~ 70 ps) and the ester groups (~ 50 ps), the more significant difference is observed in the longer time scales, where less than 1% of the water molecules remain bound to the ester groups for more than 0.7 ns whereas $\sim 9\%$ of the water molecules bound to the -NH_3^+ and phosphate groups remain for the same timescale. For the ammonium group, this is complimentary to the observation of a NOESY signal as is shown in Fig. 4. The increased retention time is likely due to the water molecules being bound to more than one PE headgroup or more than one part of the same PE headgroup.

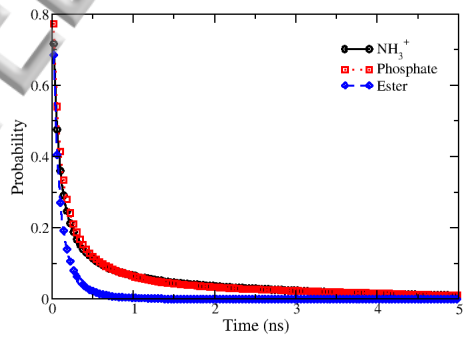

FIG. 7: Residence time distribution of water molecules around the ammonium (black), phosphate (red) and ester (blue) groups in the DOPE headgroup.

Figure 8 shows the hydration $g(r)$s for salient motifs within the DOPE head group from the EPSR fits to the neutron diffraction data and the MD simulations. The corresponding coordination numbers are shown in Table III. In all cases, the height of the $g(r)$ peaks and the coordination numbers are consistently higher for MD than EPSR. This is attributable to the aggregation of headgroups and the increased headgroup-water interactions observed for MD simulations, encouraging not only greater coordination but also enhanced excluded

This manuscript was accepted by J. Chem. Phys. Click here to see the version of record.

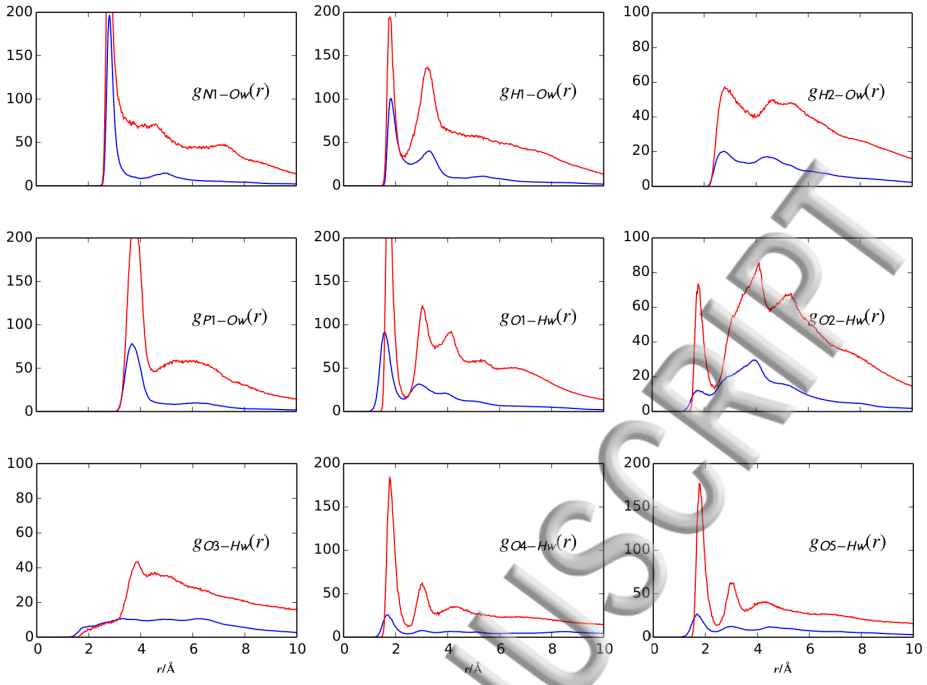

FIG. 8: The $g(r)$s for the DOPE headgroup hydration interactions in solution for the EPSR (blue) and MD (red) simulations.

	r_{min}/Å	EPSR	MD
N1-Ow	4.00	0.9	2.6
H1-Ow	2.40	0.3	0.4
H2-Ow	3.30	0.2	0.4
P1-Ow	4.50	1.2	3.4
O1-Hw	2.40	0.4	1.0
O2-Hw	2.40	0.1	0.4
O3-Hw	2.40	0.06	0.04
O4-Hw	2.40	0.1	0.7
O5-Hw	2.40	0.2	0.7

TABLE III: Coordination numbers for the DOPE headgroup hydration $g(r)$s in Figure 8.

volume effects observable in the $g(r)$s.[50] In turn, the increase in DOPE-water interactions causes a decrease in chloroform interactions with both DOPE and water in the MD simulations as compared to that from EPSR. SDMs and $g(r)$s for chloroform-water and -DOPE interactions can be found in Section V of the Supplementary Information.

Unsurprisingly, the -NH_3^+ moiety shows characteristic hydrogen bonding peaks with water at 2.82 and 1.83 Å in the g_{N1Ow}(r) and g_{H1Ow}(r) functions respectively from EPSR. These distances are marginally longer than the 2.79 and 1.77 Å distances found from the MD simulation. That water is strongly bound to this group in DOPE is consistent with the upfield shift and broadening of the H_1 peak in the ^{1}H NMR spectra in Fig. 3. The coordination numbers in Table III show that with respect to the H1-Ow hydrogen bonds that MD and EPSR are similarly coordinated. However, there is more water around this portion of the head group, over a larger distance range, with respect to the N-Ow coordination in MD compared with EPSR. This is linked with increased clustering of water around the headgroup in the MD simulations, a result also observed for the headgroup of ceramide[10].

Figure 9 (a) & (b) show the SDMs for the location of the water oxygen atoms found

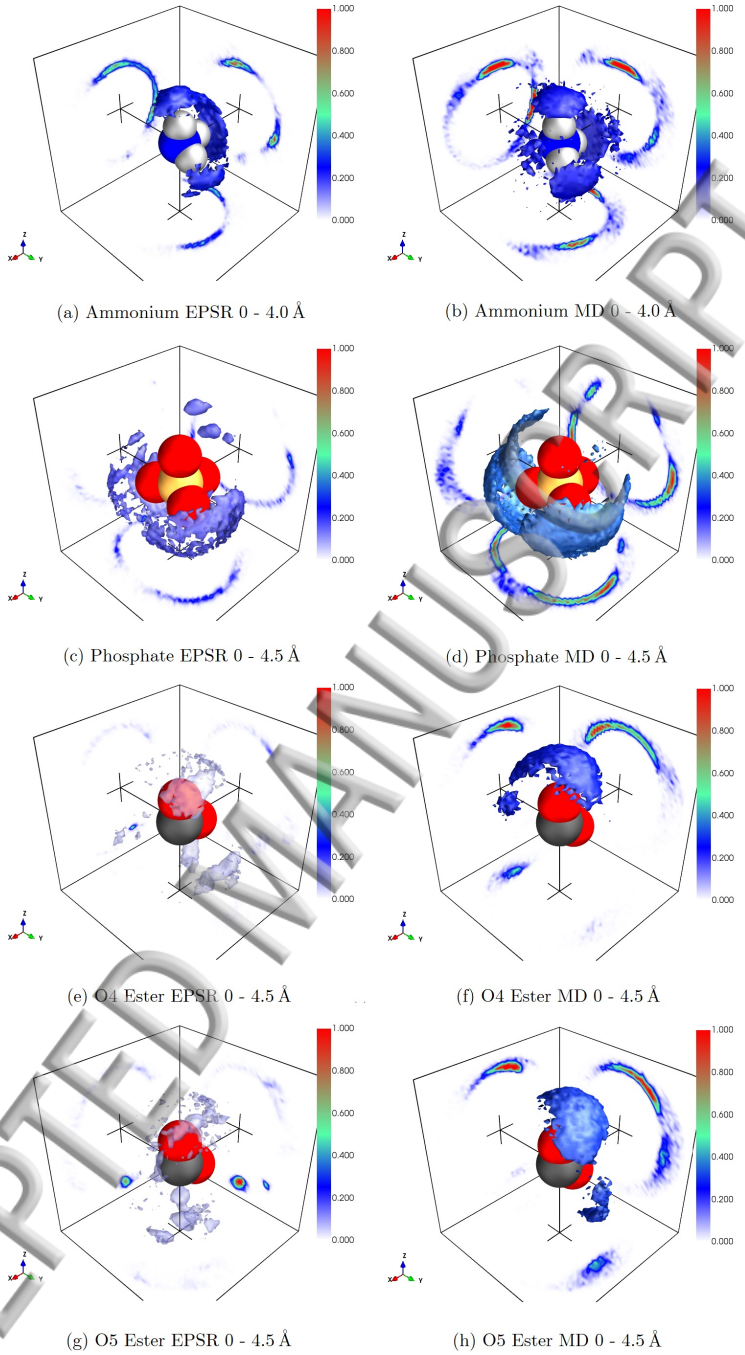

(a) Ammonium EPSR 0 - 4.0 Å

(b) Ammonium MD 0 - 4.0 Å

(c) Phosphate EPSR 0 - 4.5 Å

(d) Phosphate MD 0 - 4.5 Å

(e) O4 Ester EPSR 0 - 4.5 Å

(f) O4 Ester MD 0 - 4.5 Å

(g) O5 Ester EPSR 0 - 4.5 Å

(h) O5 Ester MD 0 - 4.5 Å

FIG. 9: SDMs for hydration through the ammonium, phosphate and ester groups. The scale bar represents the density of 40% water oxygens found in the first coordination shell per Å^3.

between 0 and 4 Å from the ammonium nitrogen in the EPSR and MD simulations, respectively. For the EPSR simulation, the water coordination is directly through the H1 atoms, with the coordination number of Ow around the N1 (0.9) being accounted for by the 0.3 Ow atoms bonding through the three H1 atoms, as listed in Table III. However, the 0.4 coordination number for the H1-Ow in the MD simulations does not account for the 2.6 Ow atoms surrounding the -NH_3^+ group, with the SDM showing that water molecules may

be interacting directly with the nitrogen atoms, in between and underneath the hydrogen atoms. This is potentially a consequence of the aggregation observed in the MD simulation.

The -CH_2- protons (H_2) directly below the -NH_3^+ group also exhibit hydration with a direct interaction peak at 2.76 Å for EPSR and 2.79 Å for MD. The H_2-Ow coordination found from EPSR suggests that on average 20% of these -CH_2- protons are bonding with water, similar to what occurs for the PC head group in solution.[11,12] Indeed, the SDMs in Figure 9 (c) & (d) suggest that water oxygens may pack on the under side of the -NH_3^+ moiety, in close proximity to the adjacent -CH_2- group.

Figure 8 also shows similar peaks for the hydration of the phosphate group. The g_{P_1Ow}(r) function has a first peak at 3.69 Å and 3.78 Å for the EPSR and MD simulations respectively, with interactions predominantly occurring through the O1 oxygens. Despite the decrease in peak intensity, the distances formed between the O1 oxygen and water hydrogen atom is consistently shorter with direct interactions with Hw atoms occurring at 1.59 Å for EPSR and 1.71 Å for MD. For EPSR, the O1-Hw coordination number is 0.4, whilst for MD it increases to 1. SDMs for the nearest neighboring oxygens around the phosphate group show that water oxygen atoms form a 'halo' around each O1 atom. The O2 oxygen atoms on the P-O-C linkage are less hydrated as has been observed for the phosphocholine headgroup in solution[12].

The least hydrated moieties of the headgroup are the ester/glycerol groups. Water is coordinated through the C=O oxygens (O4 and O5), with weak coordination through the O3 oxygen of the C-O-C linkage. Interactions between the C=O oxygens and water hydrogens occur at 1.71 Å for EPSR simulations and 1.77 Å for MD, for which the variation is likely due to the difference in packing in these simulations. In the EPSR simulation, there is slight variation in the hydration of each ester group, with the O4-Hw interaction coordination number being 0.1 and the O5-Hw value being 0.2. For the MD simulation, the hydration is higher for both esters, with each group having a coordination number of 0.7. Interestingly, SDMs from MD clearly show a difference in the arrangement of water molecules around each ester group, likely linked with the specific packing of water with respect to the rest of the chain.

Previous studies on the PC headgroup in solution have suggested that the onium group is the most hydrated, with an N-Ow coordination number of 18.6 for studies in water.[12] The extent of hydration is attributable to the size of this group, providing more sites for hydration interactions to exist through. Given the smaller size of the ammonium group for DOPE, the number of hydration interactions is comparatively less, to the degree of being slightly reduced in number compared to those of the phosphate groups.

IV. CONCLUSIONS

Through all techniques used in this study, it is apparent that water readily interacts with the polar groups of DOPE. NMR observations reveal notable changes at -NH_3^+ group, with neutron and MD studies suggesting that the hydration of the phosphate group might be comparable, if not exceeding that of the -NH_3^+ group. The lifetime for water molecules around the headgroup indicates that water remains attached to the ammonium and phosphate groups longer than the ester groups and in membranes potentially would allow for a a surface of interfacial water to be present. With increasing DOPE-water interactions comes a decrease in chloroform interactions both with water and the headgroup, seen more notably in the MD simulation.

DOPE molecules show some level of association in MD simulations, which is almost absent in EPSR simulations. The excluded volume incurred from this aggregation is apparent in the $g(r)$s for MD. Between aggregated lipids, the headgroups align so the -NH_3^+ groups interact directly with the -PO_4^- group particularly, though other combinations for instance involving the ester groups are possible. Water molecules may bridge other interactions, with 1-3 molecules between each moiety. Water molecules in these clusters are embedded within the aggregated headgroups found in the MD simulations. In chloroform, the headgroup of single

DOPE lipids can be seen to form intramolecular interactions between polar moieties. In both simulations, lipids that are not in clusters still have readily hydrated headgroups, with the residual lifetime suggesting that there is increased retention of water through interactions with the ammonium and phosphate groups. This may suggest that association of these molecules could initially be water-mediated, though upon association DOPE molecules will most predominantly interact through direct, intermolecular -NH_3^+-phosphate contacts.

In studies comparing PC and ceramide lipids in solution and membranes,[11] solution studies provided a good description of the hydration of lipids for regions closer to the outer face, with deviations appearing for moieties that would be found in the interiors of lipid membranes. The permeability of water has previously been reported as lower in PE-lipid bilayers[51] due to a correlation between permeability and the surface area per lipid.[52] The presence of increased hydration around the phosphate group in this study may mean that water could possibly embed itself further into a bilayer or membrane structure with PE lipids, depending on the lipids that neighbor them. In DOPE-rich areas, it is likely that a structural water surface forms as a result of the increased interactions that the headgroup groups are making with water. The presence of a denser water surface could potentially inhibit the diffusion of drugs through interfaces such as the BBB, particularly those drugs that are highly lipophilic and cannot dissolve in these PE-richer regions. However those drug molecules with hydrogen bonding groups that may dissolve in PE-rich regions and then displace the water bound to the PE headgroup before finally diffusing into the membrane.

V. SUPPLEMENTARY INFORMATION

Supplementary material, which has been referred to in the main text, can be found via the following link.

ACKNOWLEDGMENTS

We thank the ISIS Facility (Rutherford Appleton Laboratories, STFC, UK) for the allocation of neutron beam time, and the UK Engineering and Physical Sciences Research Council for (EP/J002615/1) and The Leverhulme Trust (RPG-2015-135) for funding. We also thank Professor Christina Redfield and Dr Nick Soffe for assistance with the NMR measurements, Drs Richard Gillams and Sam Callear for help with the neutron measurements, as well as Robert Ziolek, Paul Smith and Mateusz Bieniek for support with the MD analyses and useful discussions. Via our membership to the UK's HEC Materials Chemistry Consortium, which is funded by EPSRC (EP/L000202), this work used the ARCHER UK National Supercomputing Service (http://www.archer.ac.uk) and the UK Materials and Molecular Modelling Hub (MMM Hub) for computational resources, which is partially funded by EPSRC (EP/P020194/1) to carry out the MD simulations reported in this manuscript. Additionally, C.D.L. acknowledges the stimulating research environment provided by the EPSRC Centre for Doctoral Training in Cross-Disciplinary Approaches to Non-Equilibrium Systems (CANES, No. EP/L015854/1).

[1] A. van Dalen and B. de Kruijff, "The role of lipids in membrane insertion and translocation of bacterial proteins," Biochimica et Biophysica Acta (BBA) - Molecular Cell Research **1694**, 97 – 109 (2004), protein Export/Secretion in Bacteria.

[2] S. Suetsugu, S. Kurisu, and T. Takenawa, "Dynamic shaping of cellular membranes by phospholipids and membrane-deforming proteins," Physiological Reviews **94**, 1219–1248 (2014).

[3] J. E. Vance and G. Tasseva, "Formation and function of phosphatidylserine and phosphatidylethanolamine in mammalian cells," Biochimica et Biophysica Acta (BBA) - Molecular and Cell Biology of Lipids **1831**, 543–554 (2013).

[4] D. E. Vance, "Phospholipid methylation in mammals: from biochemistry to physiological function," Biochimica et Biophysica Acta (BBA) - Biomembranes **1838**, 1477 – 1487 (2014), membrane Structure and Function: Relevance in the Cell's Physiology, Pathology and Therapy.

[5]D. A. Pink, S. McNeila, B. Quinna, and M. J. Zuckermann, "A model of hydrogen bond formation in phosphatidylethanolamine bilayers," Biochimica et Biophysica Acta (BBA) - Biomembranes **1368**, 289–305 (1998).
[6]R. M. Venable, F. L. H. Brown, and R. W. Pastor, "Mechanical properties of lipid bilayers from molecular dynamics simulation," Chemistry and Physics of Lipids **192**, 60–74 (2015).
[7]J. L. Mikitsh and A.-M. Chacko, "Pathways for small molecule delivery to the central nervous system across the blood-brain barrier," Perspectives in Medicinal Chemistry **6**, 11–24 (2014).
[8]W. A. Banks, "Characteristics of compounds that cross the blood-brain barrier," BMC Neurology **9**, S1–S3 (2009).
[9]C. W. Gibby and J. Hall, "XCIV - the system water-chloroform," Journal of Chemical Physics **0**, 13691–693 (1931).
[10]R. J. Gillams, J. V. Busto, S. Busch, F. M. Goñi, C. D. Lorenz, and S. E. McLain, "Solvation and hydration of the ceramide headgroup in a non-polar solution." The Journal of Physical Chemistry B **119**, 128–139 (2015).
[11]R. J. Gillams, C. D. Lorenz, and S. E. McLain, "Comparative atomic-scale hydration of the ceramide and phosphocholine headgroup in solution and bilayer environments," The Journal of Chemical Physics **144**, 225101 (2016).
[12]F. Foglia, M. J. Lawrence, C. D. Lorenz, and S. E. McLain, "On the hydration of the phosphocholine headgroup in aqueous solution." The Journal of Chemical Physics **133**, 145103 (2010).
[13]A. P. Dabkowska, F. Foglia, M. J. Lawrence, C. D. Lorenz, and S. E. McLain, "On the solvation structure of dimethylsulfoxide/water around the phosphatidylcholine head group in solution." The Journal of Chemical Physics **135**, 225105 (2011).
[14]N. H. Rhys, M. A. Al-Badri, R. M. Ziolek, R. J. Gillams, L. E. Collins, M. Lawrence, C. D. Lorenz, and S. E. McLain, "On the solvation of the phosphocholine headgroup in an aqueous propylene glycol solution," The Journal of Chemical Physics **48**, 1351032 (2018).
[15]H. E. Gottlieb, V. Kotlyar, and A. Nudelman, "Nmr chemical shifts of common laboratory solvents as trace impurities," The Journal of Organic Chemistry **62**, 7512–7515 (1997).
[16]A. K. Soper, "GudrunN and GudrunX: Programs for Correcting Raw Neutron and X-ray Diffraction Data to Differential Scattering Cross Section," RAL Report **RAL-TR-201** (2011).
[17]V. F. Sears, "Neutron scattering lengths and cross sections," Neutron News **3**, 26–37 (1992).
[18]S. E. McLain, C. J. Benmore, J. E. Siewenie, J. Urquidi, and J. F. C. Turner, "On the structure on hydrogen fluoride," Angewandte Chemie International Edition **43**, 1952–1955 (2004).
[19]A. K. Soper, "Partial structure factors from disordered materials diffraction data: An approach using empirical potential structure refinement," Physical Review B **72**, 104204–104215 (2005).
[20]A. K. Soper, "Empirical potential Monte Carlo simulation of fluid structure," Chemical Physics **202**, 295–306 (1996).
[21]A. J. Johnston, S. Busch, L. C. Pardo, S. K. Callear, P. C. Biggin, and S. E. McLain, "On the atomic structure of cocaine in solution," Physical Chemistry Chemical Physics **18**, 991–999 (2016).
[22]J. J. Shephard, S. K. Callear, S. Imberti, J. S. O. Evans, and C. G. Salzmann, "Microstructures of negative and positive azeotropes," Physical Chemistry Chemical Physics **18**, 19227–19235 (2016).
[23]N. Steinke, R. J. Gillams, L. C. Pardo, C. D. Lorenz, and S. E. McLain, "Atomic scale insights into ureapeptide interactions in solution," Physical Chemistry Chemical Physics **18**, 3862–3870 (2016).
[24]N. Steinke, A. Genina, C. D. Lorenz, and S. E. McLain, "Salt interactions in solution prevent direct association of urea with a peptide backbone," The Journal of Physical Chemistry B **121**, 1866–1876 (2017).
[25]N. H. Rhys, R. J. Gillams, L. E. Collins, S. K. Callear, M. J. Lawrence, and S. E. McLain, "On the structure of an aqueous propylene glycol solution," The Journal of Chemical Physics **145**, 224504 (2016).
[26]A. Silva-Santisteban, N. Steinke, A. J. Johnston, G. N. Ruiz, L. Carlos Pardo, and S. E. McLain, "On the structure of prilocaine in aqueous and amphiphilic solutions," Physical Chemistry Chemical Physics **19**, 12665–12673 (2017).
[27]N. H. Rhys, F. Bruni, S. Imberti, S. E. McLain, and M. A. Ricci, "Glucose and mannose: A link between hydration and sweetness," The Journal of Physical Chemistry B **121**, 7771–7776 (2017).
[28]M. Gilmore, L. M. Moura, A. H. Turner, M. Swadzba-Kwasny, S. K. Callear, J. A. McCune, O. A. Scherman, and J. D. Holbrey, "A comparison of choline:urea and choline:oxalic acid deep eutectic solvents at 338 k," The Journal of Chemical Physics **148**, 193823 (2018).
[29]A. H. Turner, S. Imberti, M. Swadzba-Kwasny, and J. D. Holbrey, "Applying neutron diffraction with isotopic substitution to the structure and proton-transport pathways in protic imidazolium bis(trifluoromethyl)sulfonylimide ionic liquids," The Journal of Chemical Physics **148**, 193823 (2018).
[30]O. S. Hammond, D. T. Bowron, and K. J. Edler, "The effect of water upon deep eutectic solvent nanostructure: An unusual transition from ionic mixture to aqueous solution," Angewandte Chemie International Edition **129**, 99149917 (2017).
[31]S. Lenton, N. H. Rhys, J. J. Towey, A. K. Soper, and L. Dougan, "Highly compressed water structure observed in a perchlorate aqueous solution," Nature Communications **8**, 919 (2017).
[32]J. B. Klauda, R. M. Venable, J. A. Freites, J. W. O'Connor, D. J. Tobias, C. Mondragon-Ramirez, I. Vorobyov, A. D. MacKerell Jr., , and R. W. Pastor, The Journal of Physical Chemistry B **114**, 7830–7843 (2010).

[33]S. Jo, T. Kim, V. G. Iyer, and W. Im, "CHARMM-GUI: A Web-based graphical user interface for CHARMM," Journal of Computational Chemistry **29**, 1859 – 1865 (2008).
[34]E. L. Wu, X. Cheng, S. Jo, H. Rui, K. C. Song, E. M. Dávila-Contreras, Y. Qi, J. Lee, V. Monje-Galvan, R. M. Venable, J. B. Klauda, and W. Im, "CHARMM-GUI Membrane Builder Toward Realistic Biological Membrane Simulations," Journal of Computational Chemistry **35**, 1997 – 2004 (2014).
[35]H. J. C. Berendsen, J. R. Grigera, and T. P. Straatsma, "The missing term in effective pair potentials," The Journal of Physical Chemistry **91**, 6269–6271 (1987).
[36]W. L. Jorgensen, D. S. Maxwell, and J. Tirado-Rives, "Development and testing of the opls all-atom force field on conformational energetics and properties of organic liquids," Journal of the American Chemical Society **118**, 1122511236 (1996).
[37]W. L. Jorgensen, J. Chandrasekhar, J. D. Madura, R. W. Impey, and M. L. Klein, "Comparison of simple potential functions for simulating liquid water," The Journal of Chemical Physics **79**, 926–935 (1983).
[38]W. E. Reiher, Theoretical Studies of Hydrogen Bonding, Ph.D. thesis (1985).
[39]C. Caleman, P. J. van Maaren, M. Hong, J. S. Hub, L. T. Costa, and D. van der Spoel, "Force Field Benchmark of Organic Liquids: Density, Enthalpy of Vaporization, Heat Capacities, Surface Tension, Isothermal Compressibility, Volumetric Expansion Coefficient, and Dielectric Constant." Journal of Chemical Theory and Computation **8**, 61–74 (2012).
[40]J.-P. Ryckaert, G. Ciccotti, and H. J. Berendsen, "Numerical integration of the cartesian equations of motion of a system with constraints: Molecular dynamics of n-alkanes," Journal of Computational Physics **23**, 327–341 (1977).
[41]S. Plimpton, "Fast parallel algorithms for short-range molecular dynamics," J. Comp. Phys. **117**, 1–19 (1995).
[42]R. W. Hockney and J. W. Eastwood, Computer Simulation Using Particles (Adam Hilger, New York, 1988).
[43]R. J. Gillams, C. D. Lorenz, and S. E. McLain, "On the hydration and conformation of cocaine in solution," Chemical Physics Letters **676**, 58–64 (2017).
[44]A. A. Hagberg, D. A. Schult, and P. Swart, "Exploring network structure, dynamics, and function using networkx," in In Proceedings of the 7th Python in Science Conference (SciPy2008), edited by G. Varoquaux, T. Vaught, and J. Millman (Pasadena, CA USA, 2008) pp. 11–15.
[45]P. M. Smith, R. M. Ziolek, E. Gazzarini, and D. M. O. C. D. Lorenz, "On the interaction of hyaluronic acid with synovial fluid lipid membranes," Physical Chemistry Chemical Physics , submitted (2018).
[46]"https://gcm.upc.edu/en/members/luis-carlos/angula/angula,".
[47]S. Busch, C. D. Lorenz, J. Taylor, L. C. Pardo, and S. E. McLain, "Short-range interactions of concentrated proline in aqueous solution," The Journal of Physical Chemistry B **118**, 14267–14277 (2014).
[48]A. J. Sodt and R. W. Pastor, "Bending free energy from simulation: correspondence of planar and inverse hexagonal lipid phases," Biophysical Journal **104**, 2202–2211 (2013).
[49]A. J. Sodt and R. W. Pastor, "Molecular modeling of lipid membrane curvature induction by a peptide: More than simply shape," Biophysical Journal **106**, 1958–1969 (2014).
[50]A. K. Soper, "The excluded volume effect in confined fluids and liquid mixtures," Journal of Physics: Condensed Matter **9**, 2399 (1997).
[51]J. C. Mathai, S. Tristam-Nagle, J. F. Nagle, and M. L. Zeidel, "Structural determinants of water permeability through the lipid membrane," Journal of General Physiology **131**, 69–76 (2008).
[52]J. F. Nagle, J. C. Mathai, M. L. Zeidel, S. Tristam-Nagle, and N, "Theory of passive permeability through lipid bilayers," Journal of General Physiology **131**, 77–85 (2008).

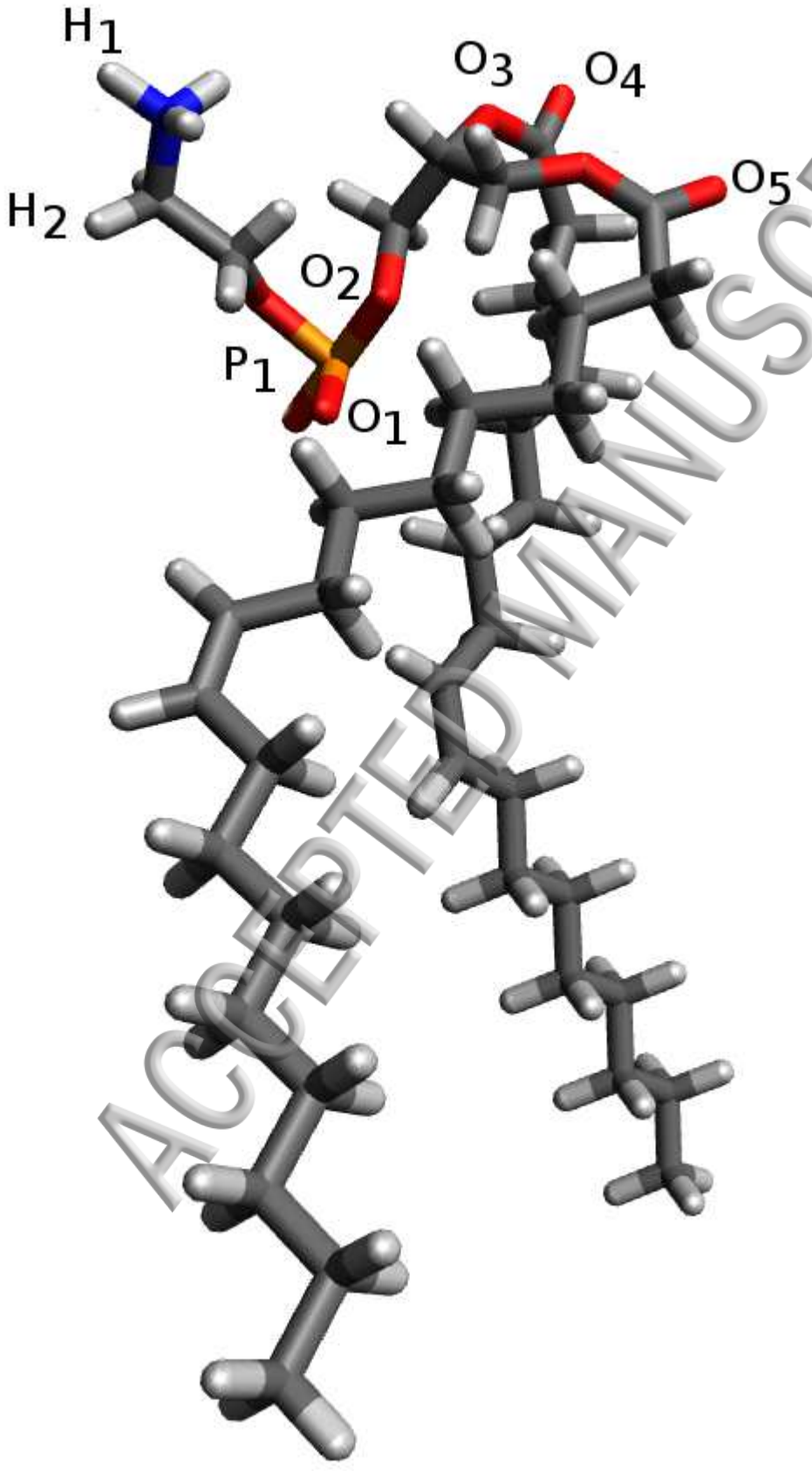

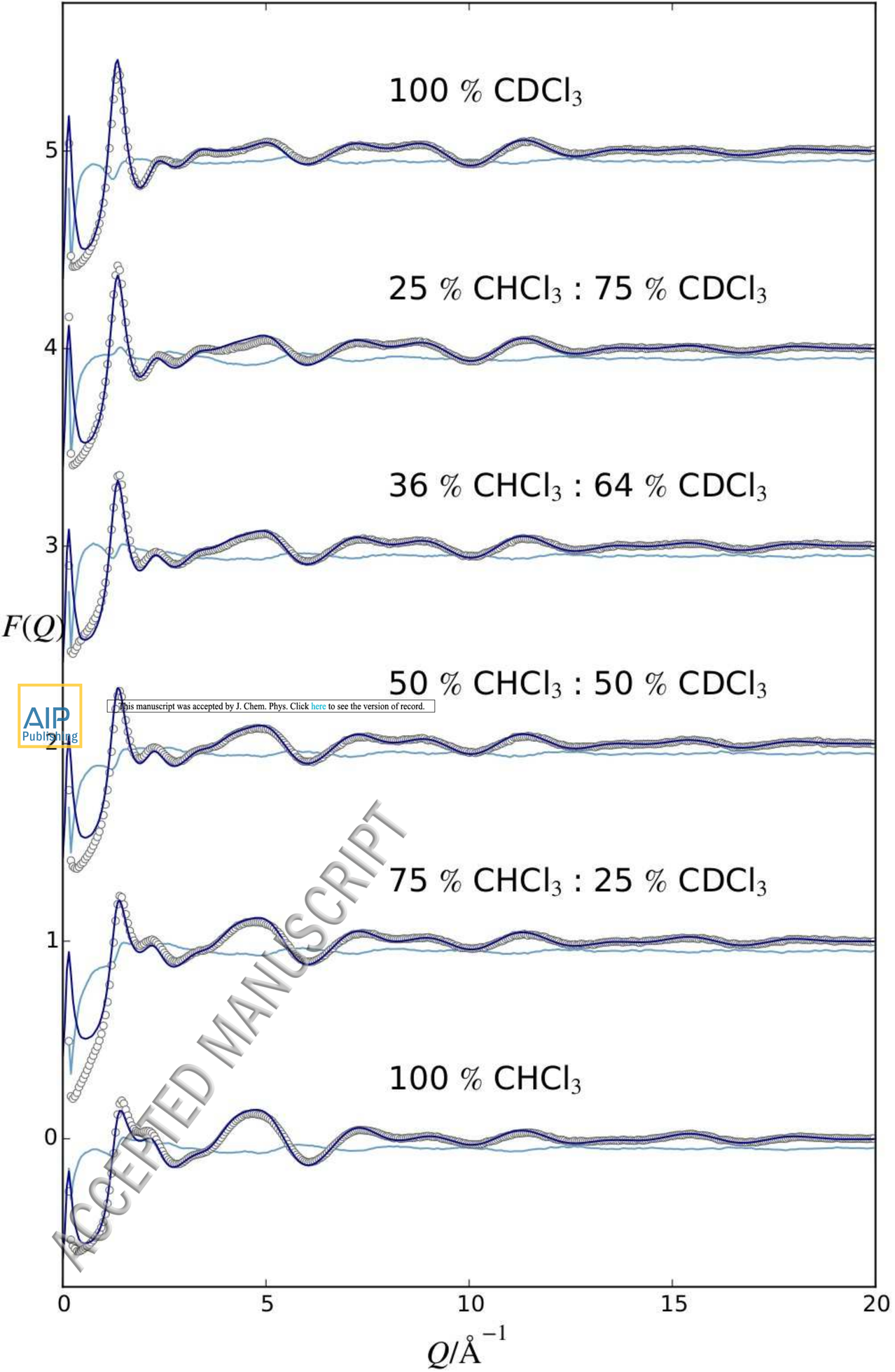

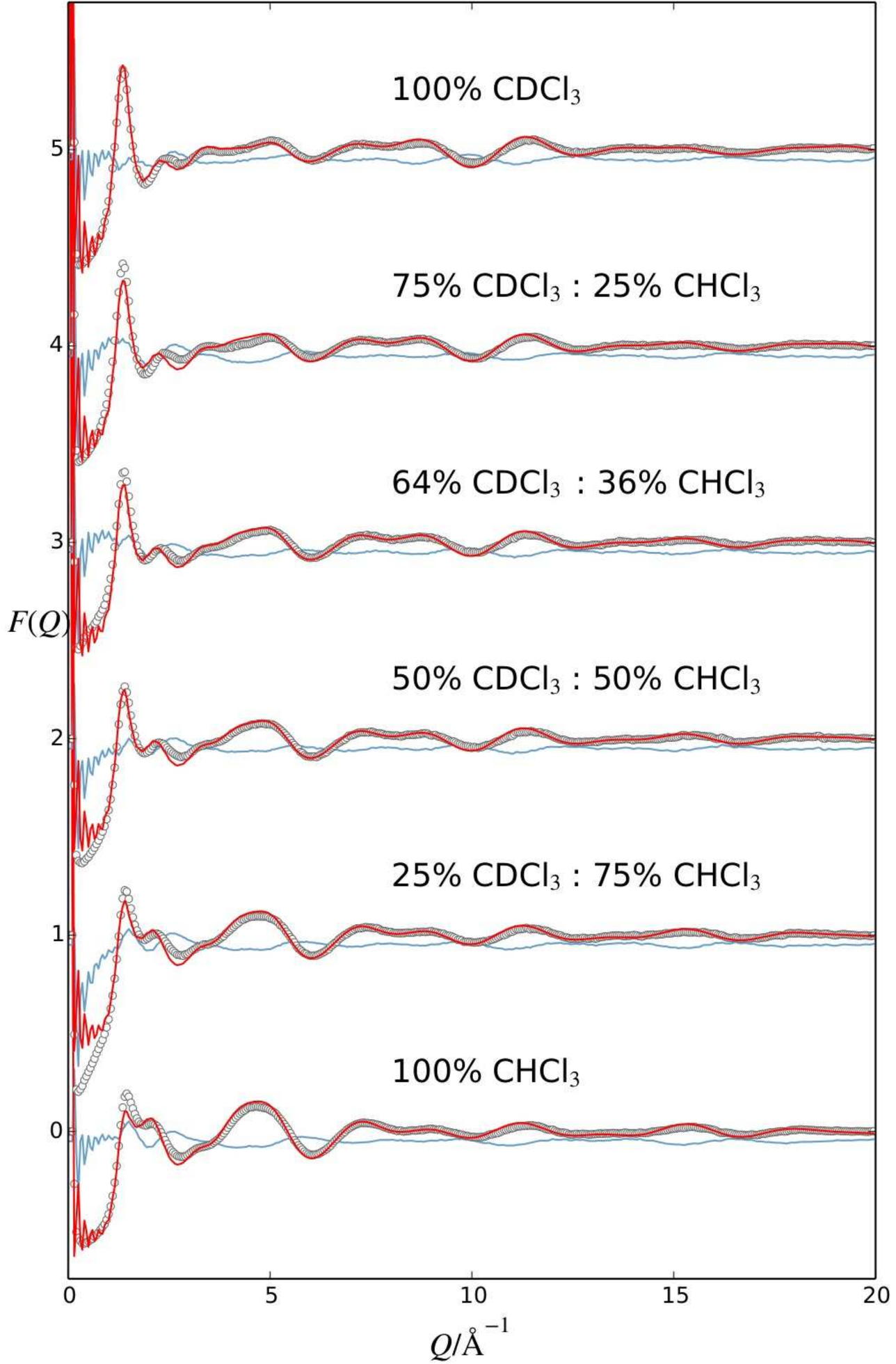

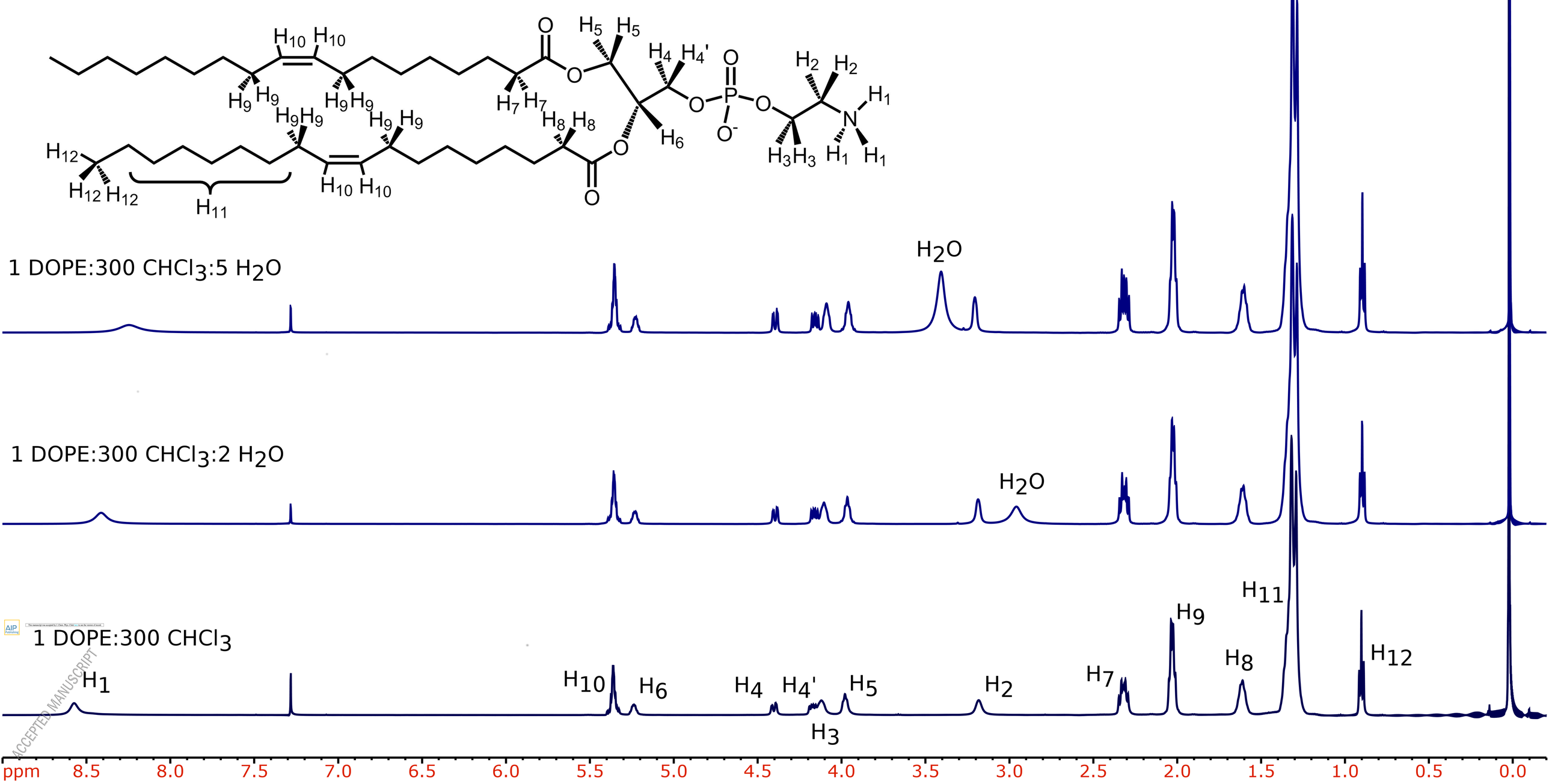

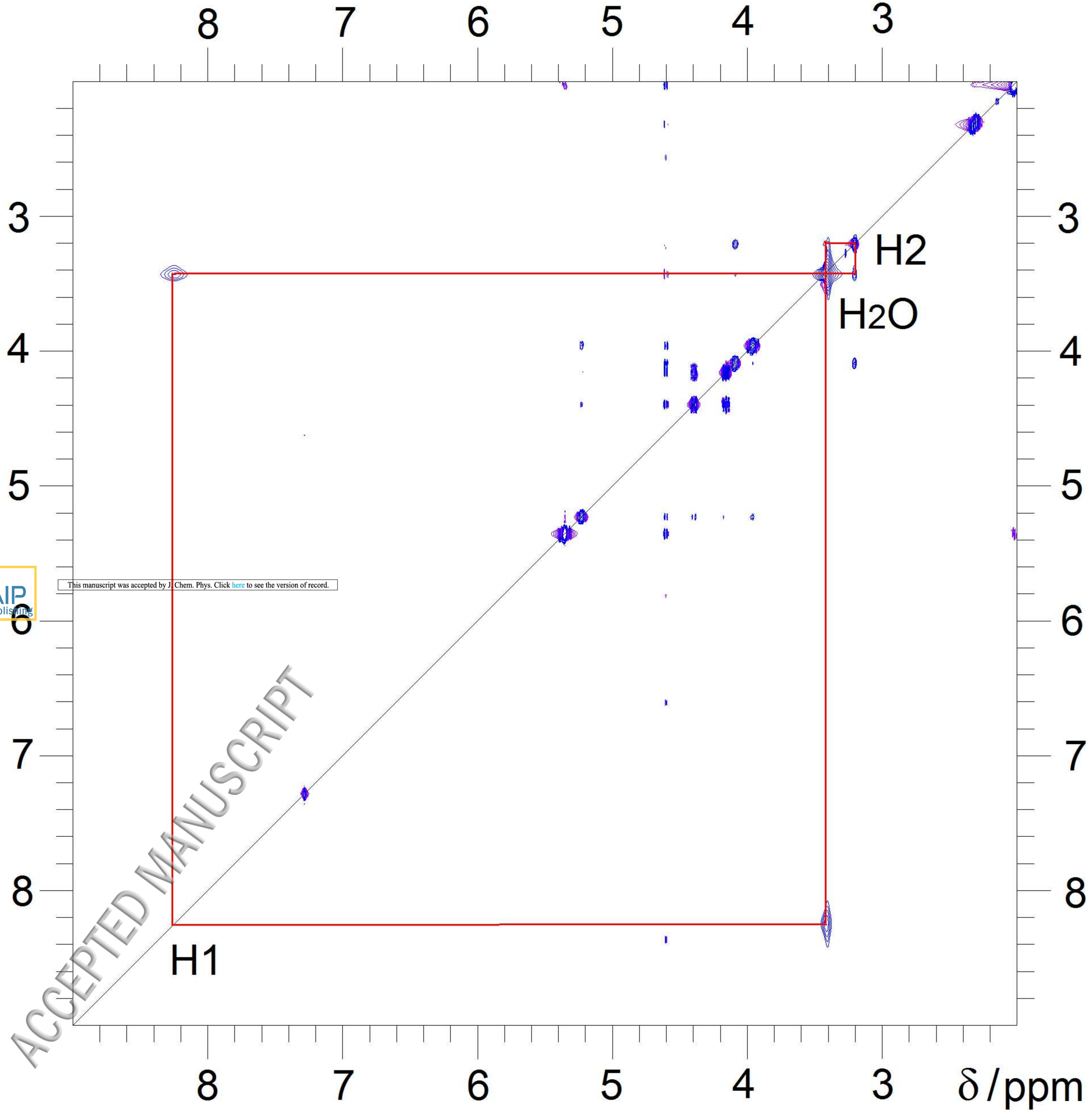

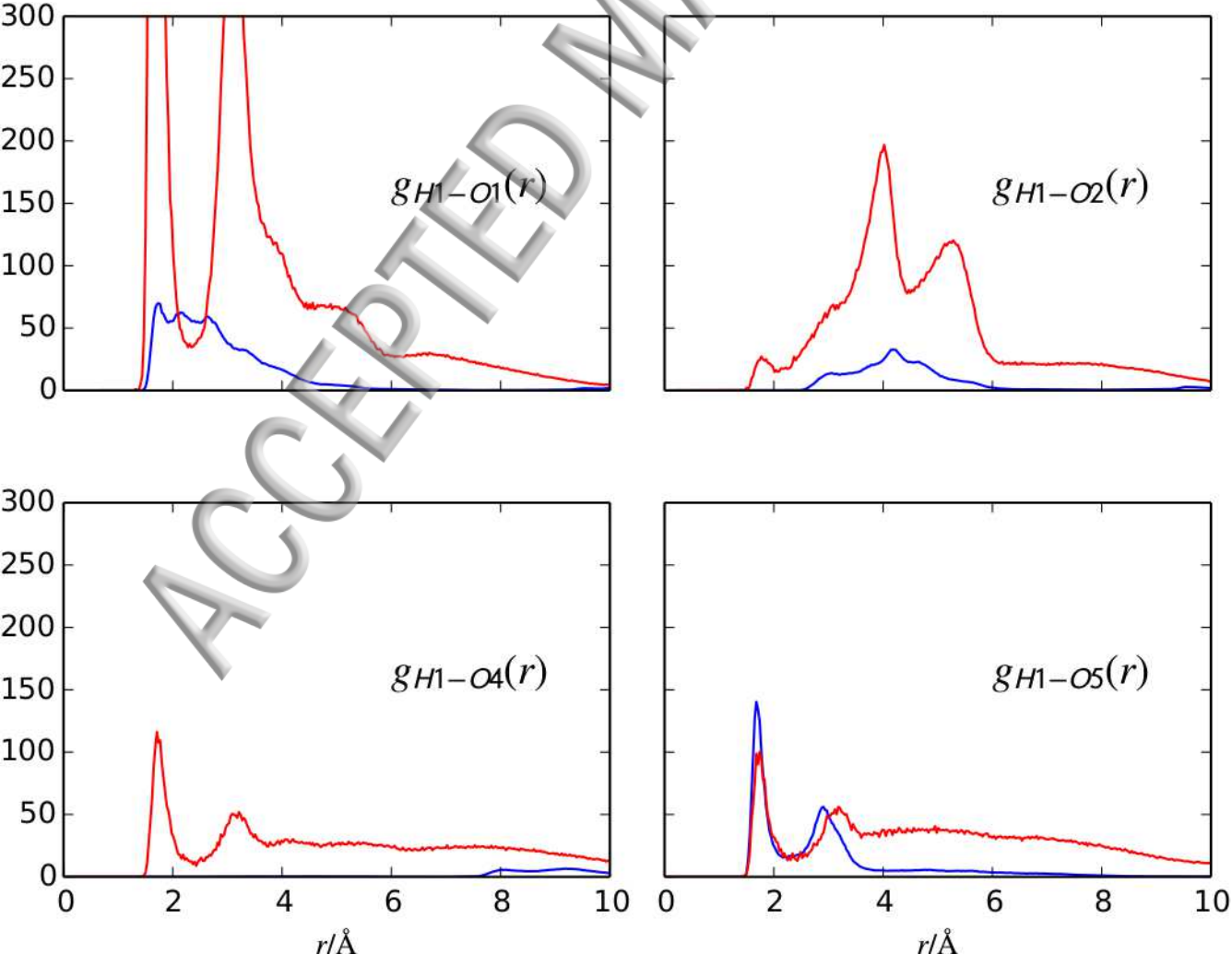
$g_{H1-O1}(r)$
$g_{H1-O2}(r)$
$g_{H1-O4}(r)$
$g_{H1-O5}(r)$
300
250
200
150
100
50
0
0
2
4
6
8
10
r/Å

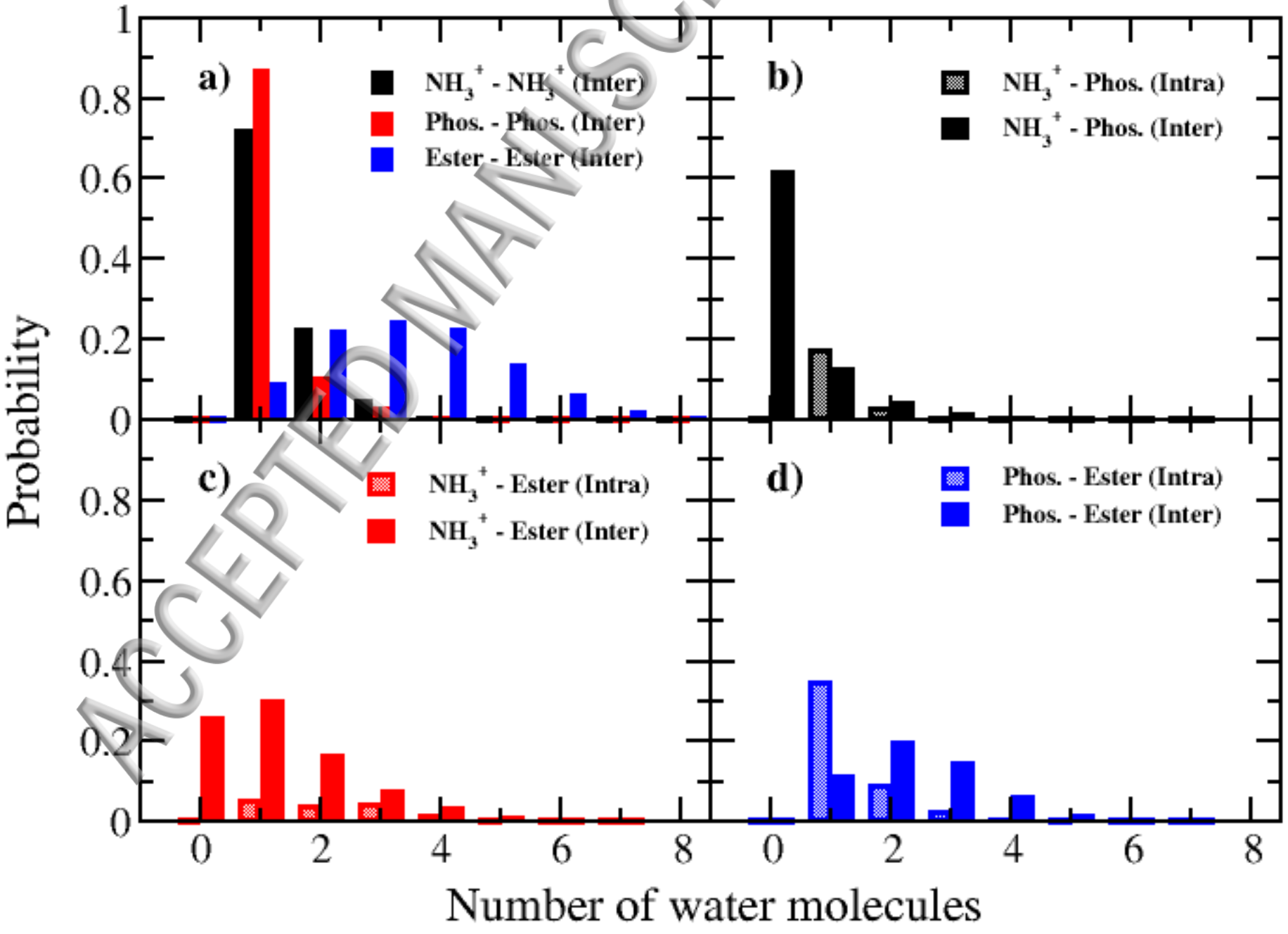

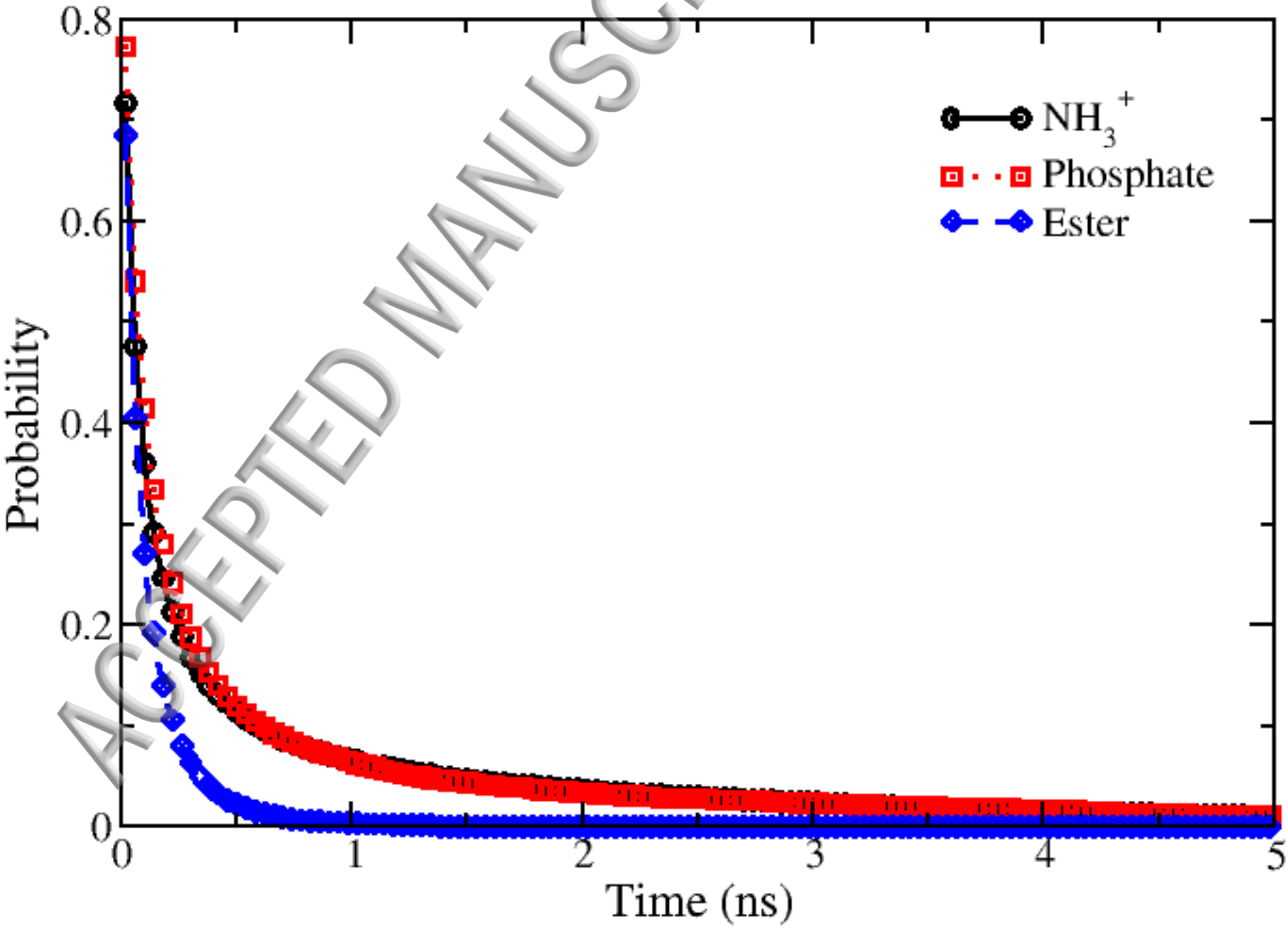

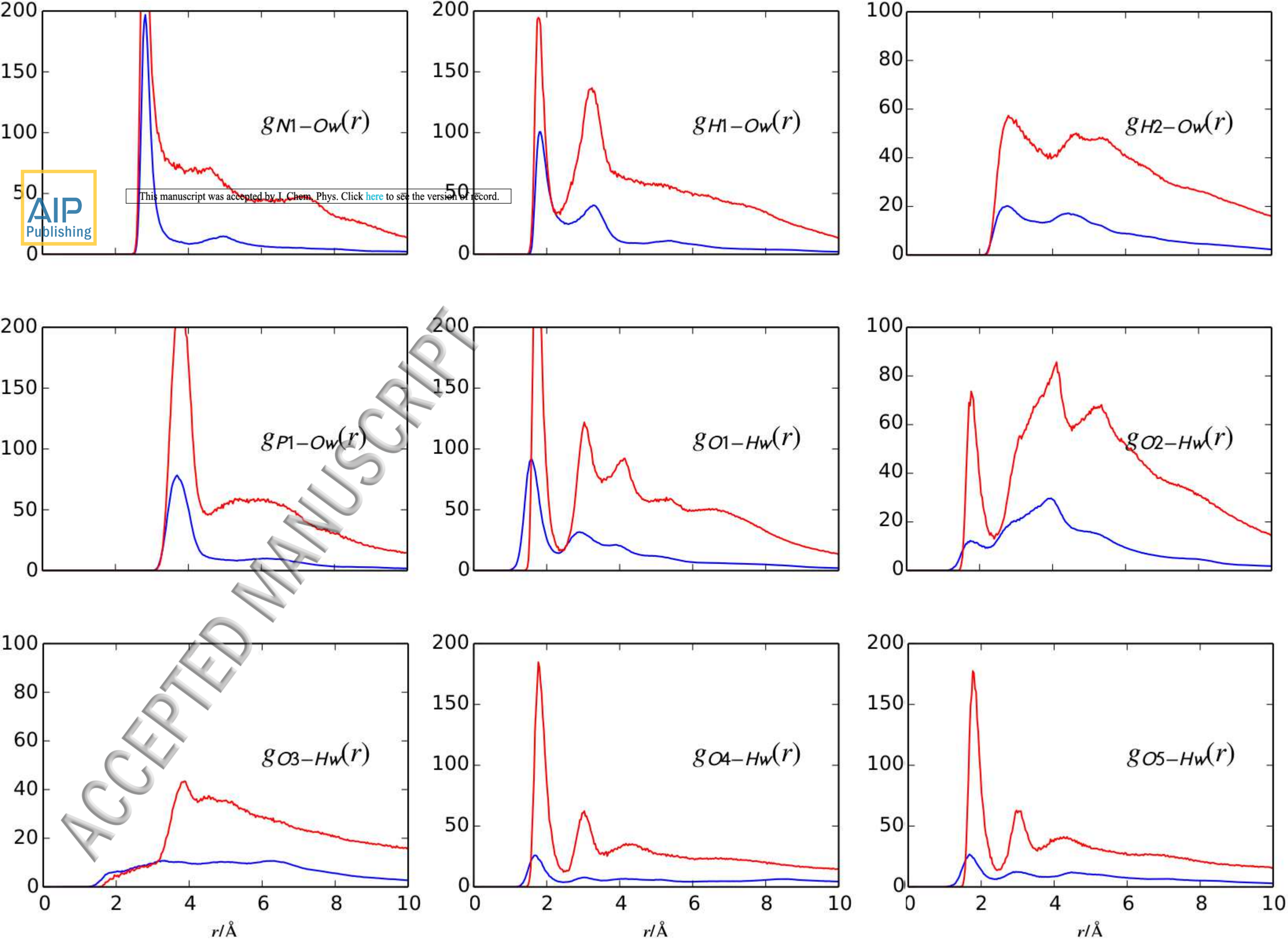

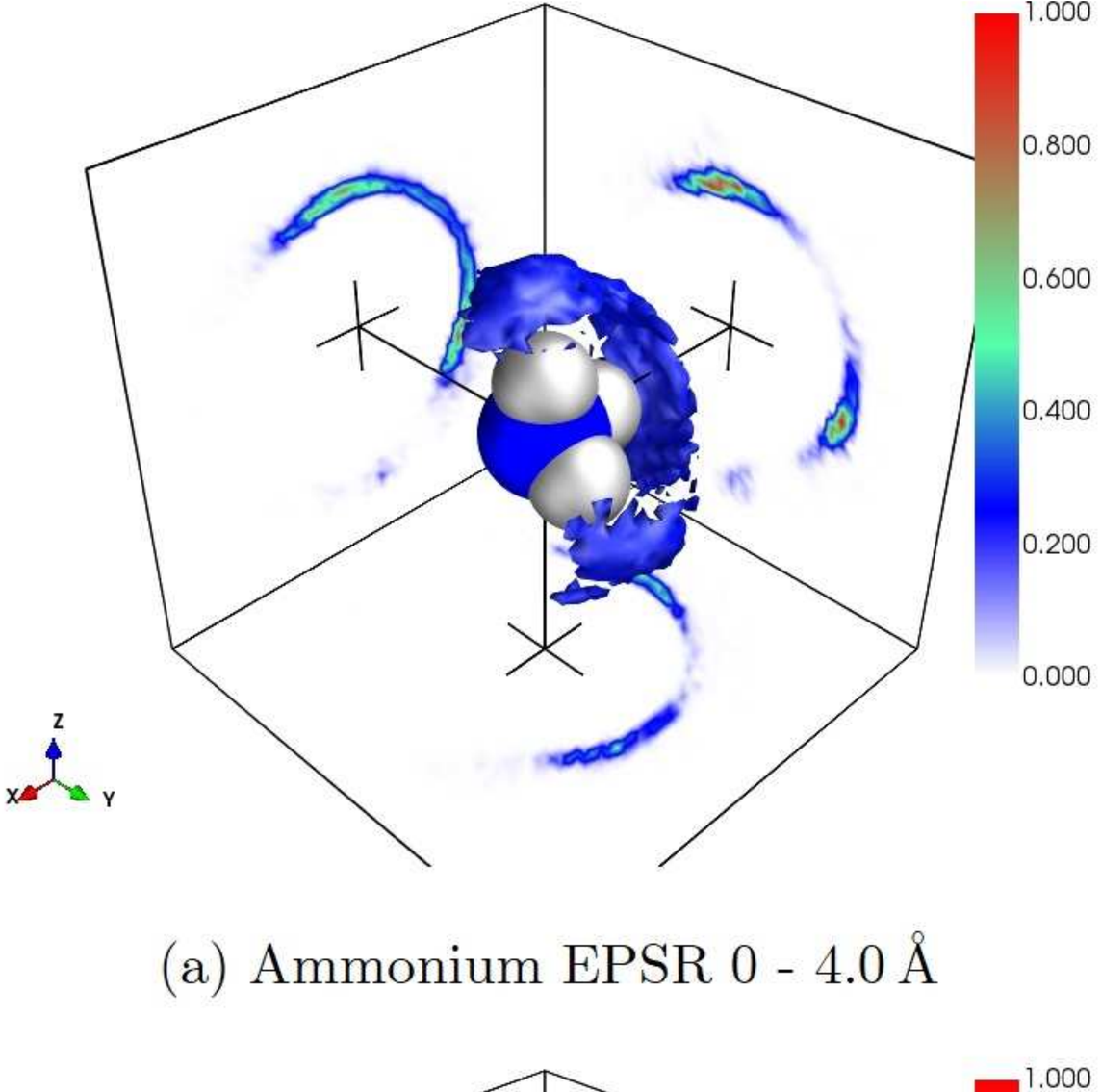

(a) Ammonium EPSR 0 - 4.0 Å

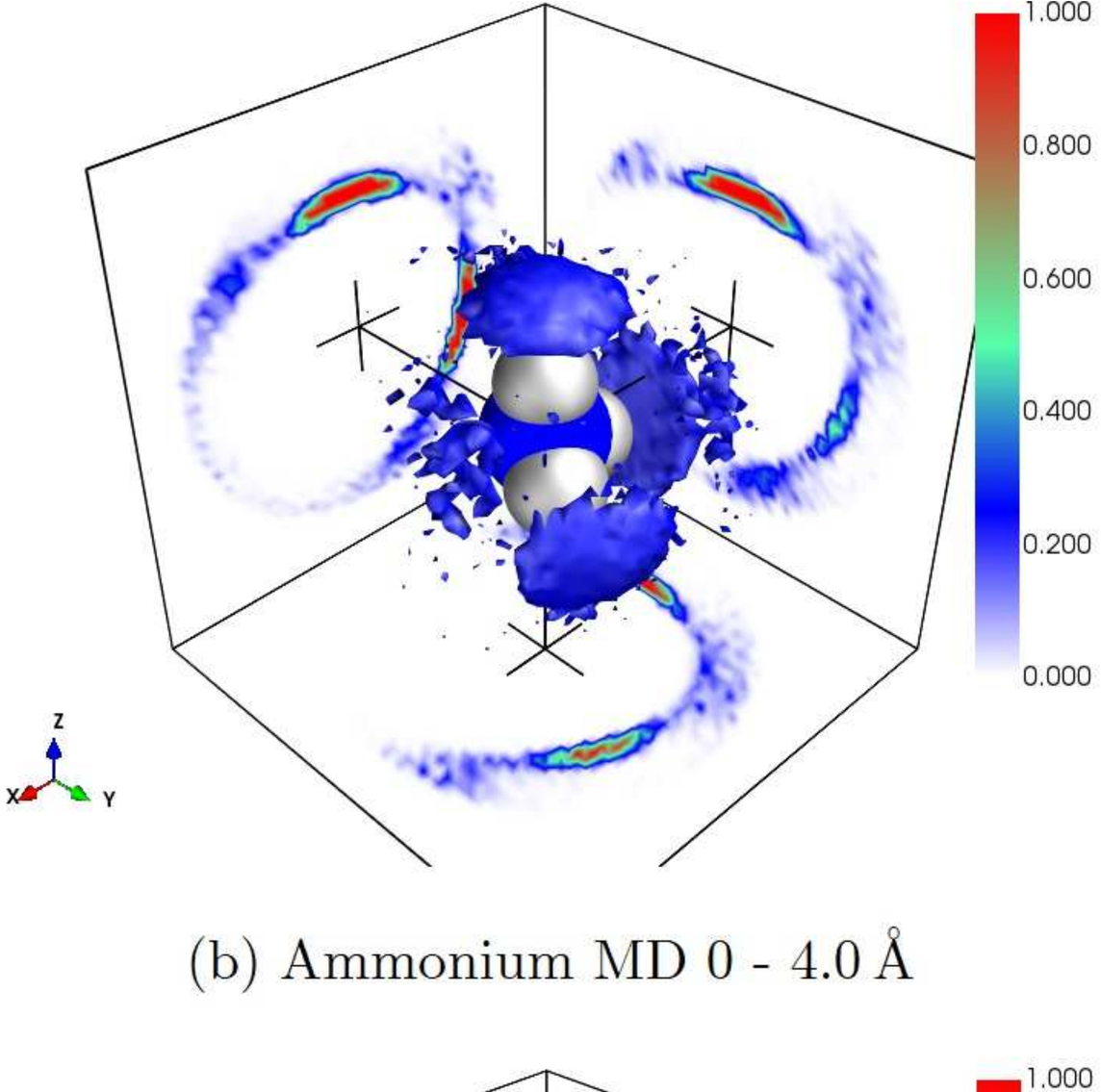

(b) Ammonium MD 0 - 4.0 Å

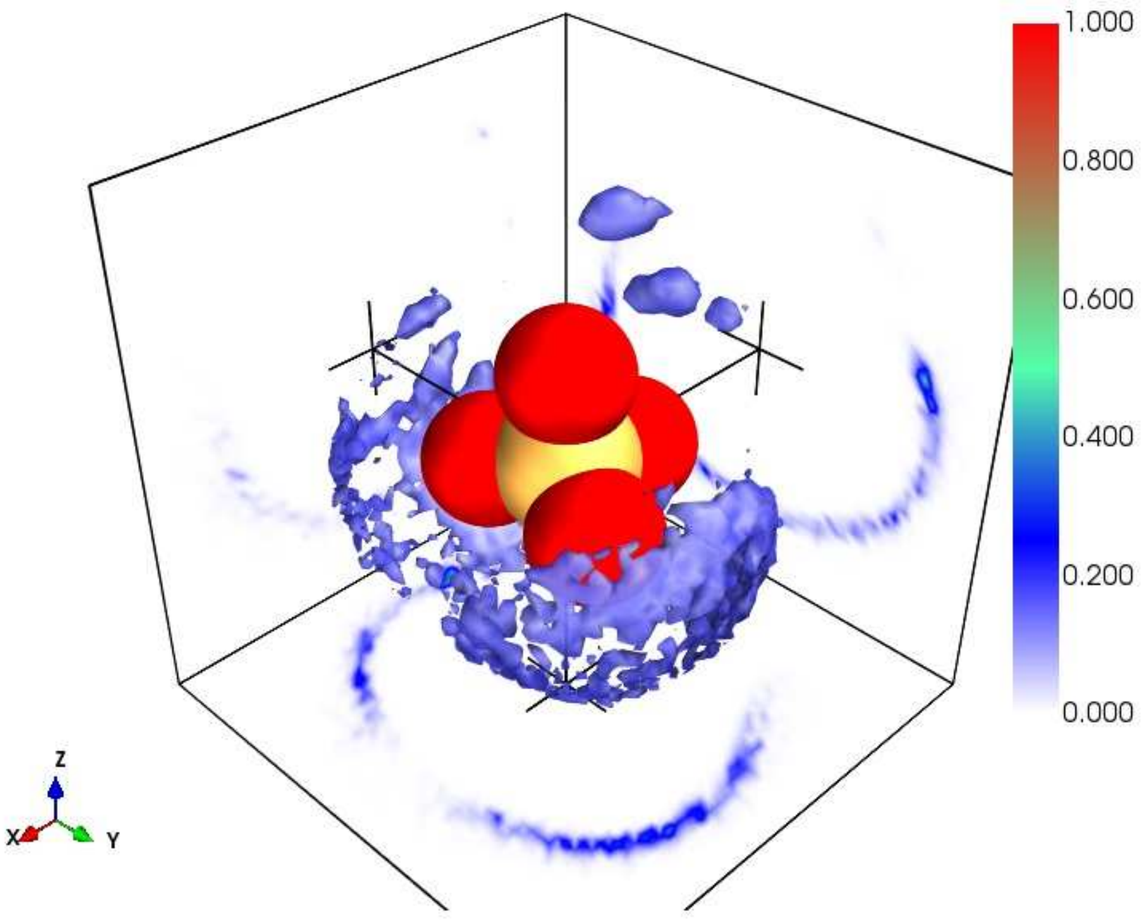

(c) Phosphate EPSR 0 - 4.5 Å

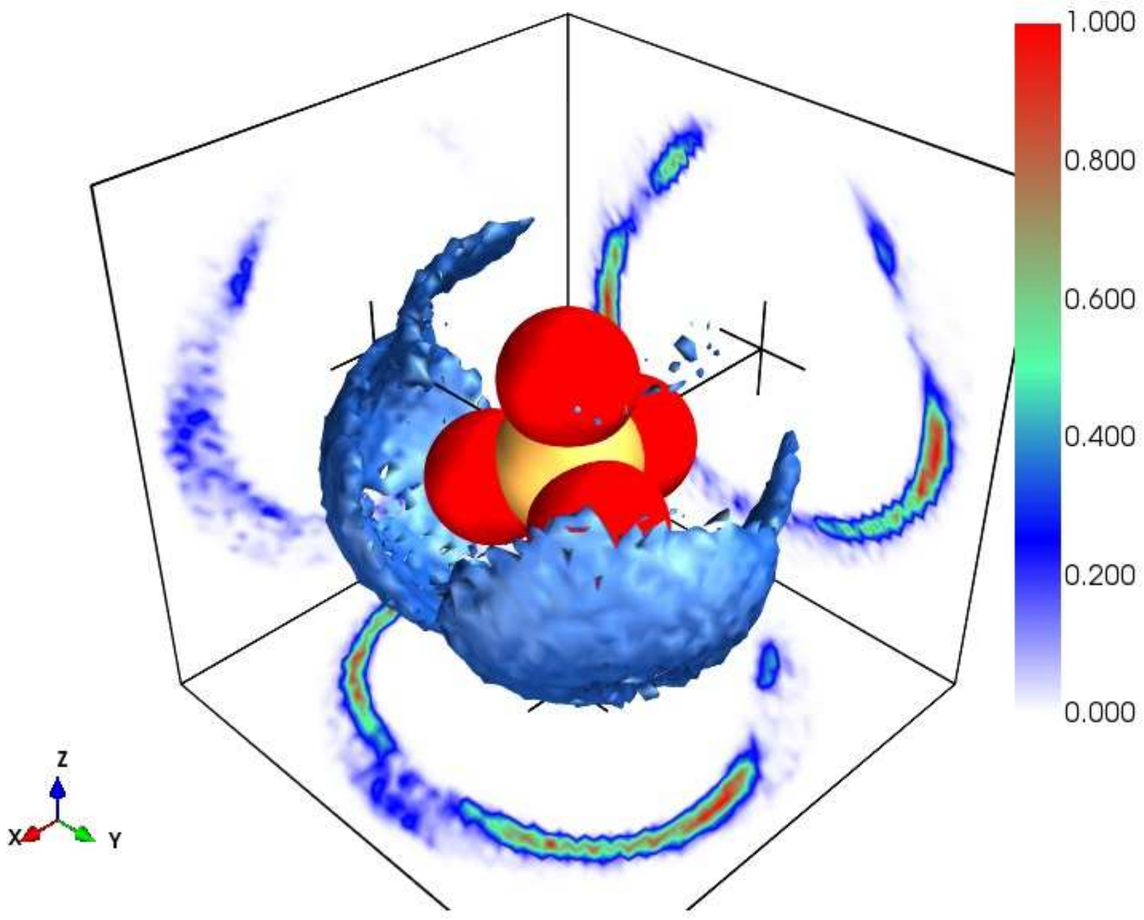

(d) Phosphate MD 0 - 4.5 Å

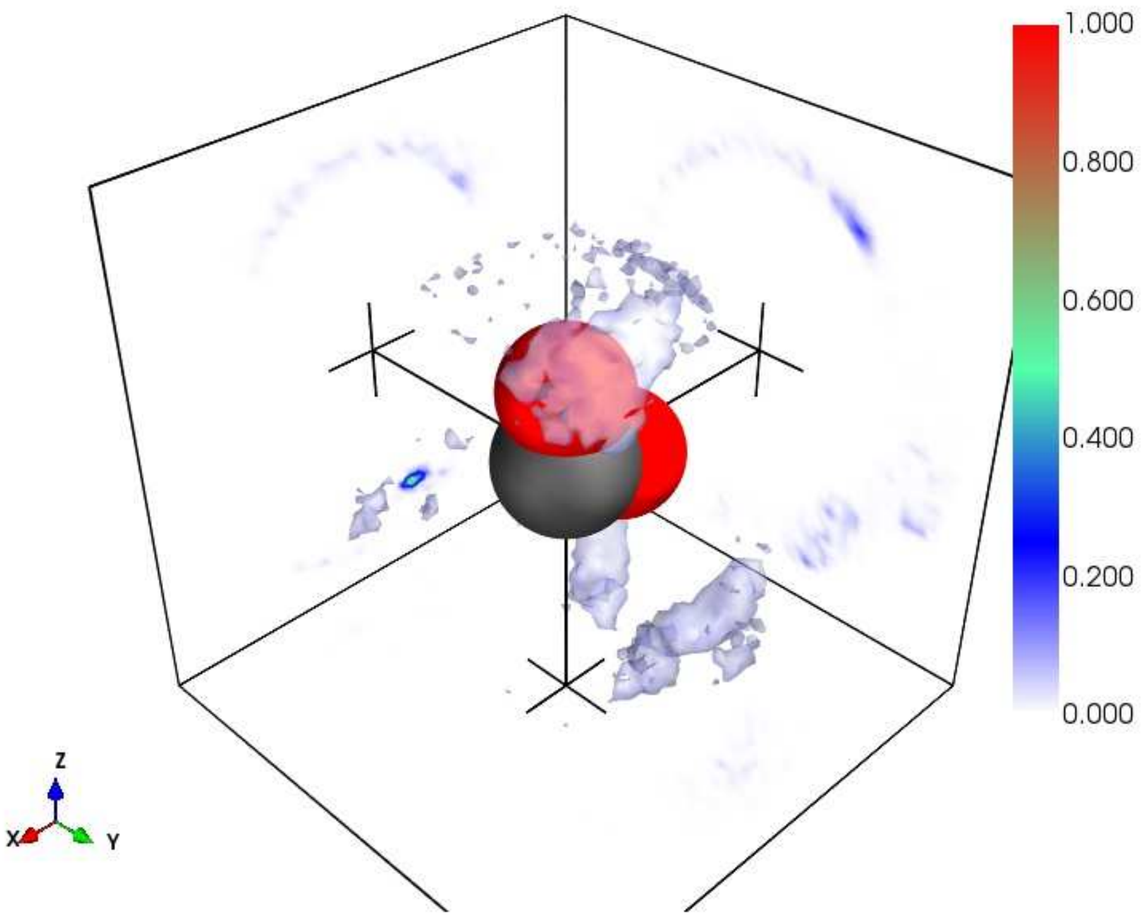

(e) O4 Ester EPSR 0 - 4.5 Å

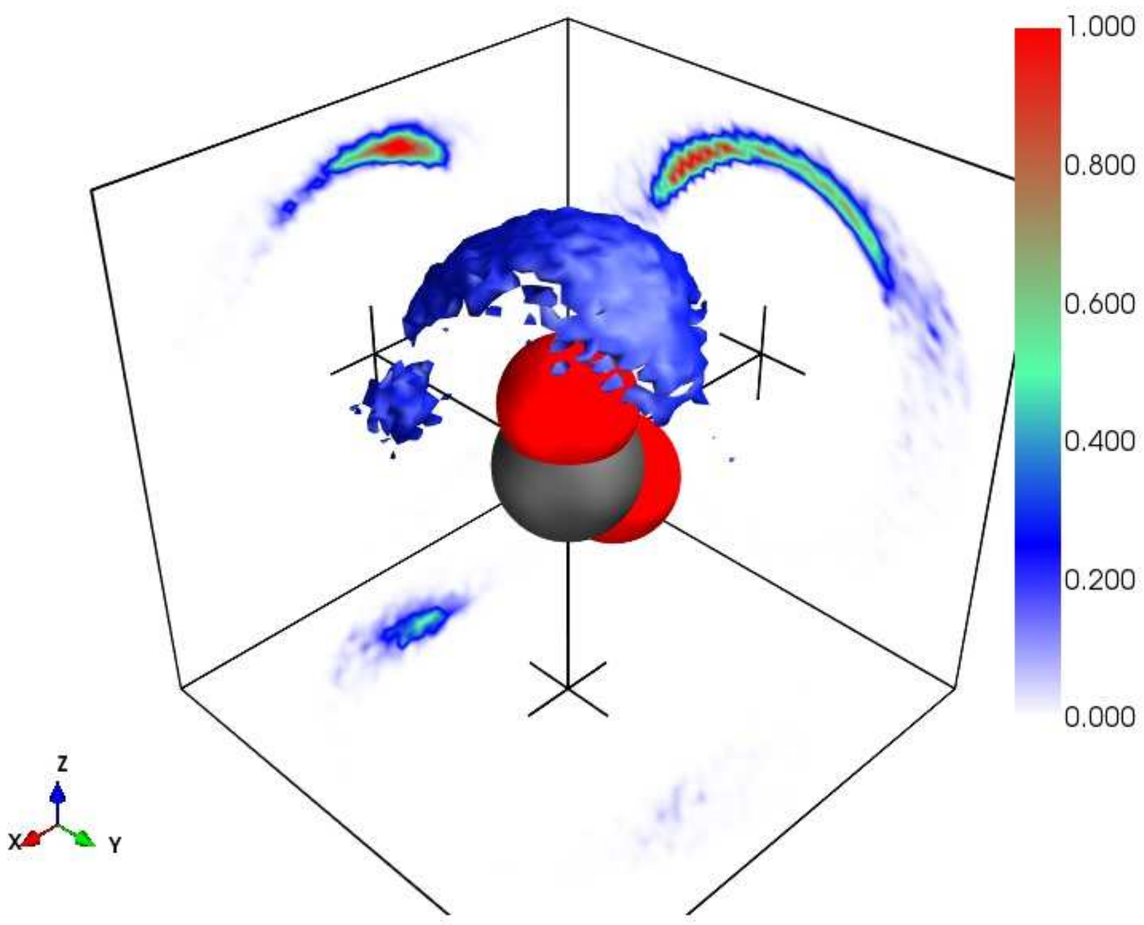

(f) O4 Ester MD 0 - 4.5 Å

(g) O5 Ester EPSR 0 - 4.5 Å

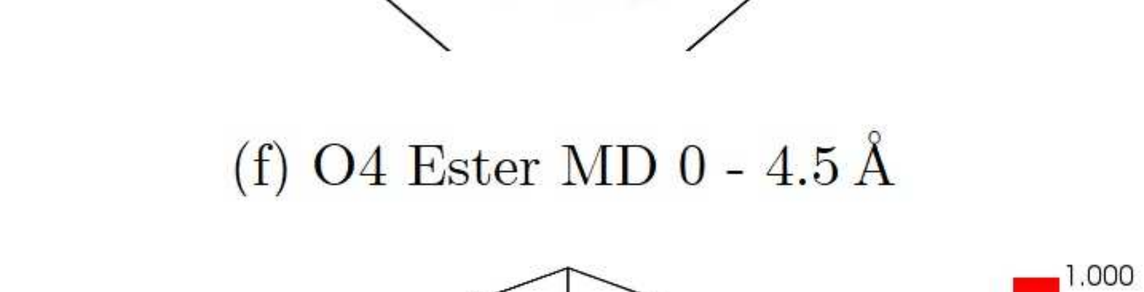

(h) O5 Ester MD 0 - 4.5 Å